



## A method for aggregating external operating conditions in multi-generation system optimization models

Lythcke-Jørgensen, Christoffer Ernst; Münster, Marie; Ensinas, Adriano Viana; Haglind, Fredrik

*Published in:*  
Applied Energy

*Link to article, DOI:*  
[10.1016/j.apenergy.2015.12.050](https://doi.org/10.1016/j.apenergy.2015.12.050)

*Publication date:*  
2016

*Document Version*  
Peer reviewed version

[Link back to DTU Orbit](#)

*Citation (APA):*  
Lythcke-Jørgensen, C. E., Münster, M., Ensinas, A. V., & Haglind, F. (2016). A method for aggregating external operating conditions in multi-generation system optimization models. *Applied Energy*, 166, 59-75.  
<https://doi.org/10.1016/j.apenergy.2015.12.050>

---

### General rights

Copyright and moral rights for the publications made accessible in the public portal are retained by the authors and/or other copyright owners and it is a condition of accessing publications that users recognise and abide by the legal requirements associated with these rights.

- Users may download and print one copy of any publication from the public portal for the purpose of private study or research.
- You may not further distribute the material or use it for any profit-making activity or commercial gain
- You may freely distribute the URL identifying the publication in the public portal

If you believe that this document breaches copyright please contact us providing details, and we will remove access to the work immediately and investigate your claim.

# 1 A method for aggregating external 2 operating conditions in multi-generation 3 plant optimization models

---

4 Adriano Viana Ensinas<sup>a</sup>, Fredrik Haglind<sup>b</sup>, Marie Münster<sup>c</sup>, Christoffer Lythcke-Jørgensen<sup>b\*</sup>

5 <sup>a</sup> École Polytechnique Fédérale de Lausanne, Industrial Process and Energy Systems Engineering, Rue de  
6 l'Industrie 17, Case Postale 440, CH-1951 Sion

7 <sup>b</sup> Technical University of Denmark, Mechanical Engineering, Nils Koppels Allé 403, DK-2800 Kgs. Lyngby

8 <sup>c</sup> Technical University of Denmark, Management Engineering, Produktionstorvet 424, DK-2800 Kgs. Lyngby

9 \* Corresponding author. +45 30 42 72 00. Email: [celjo@mek.dtu.dk](mailto:celjo@mek.dtu.dk).

## 10 **Abstract**

11 This paper presents a novel, simple method for reducing external operating condition datasets to be used  
12 in multi-generation plant optimization models. The method, called the Characteristic Operating Pattern  
13 (CHOP) method, is a visually-based aggregation method that clusters reference data based on parameter  
14 values rather than time of occurrence, thereby preserving important information on short-term relations  
15 between the relevant operating parameters. This is opposed to commonly used methods where data are  
16 averaged over chronological periods (months or years), and extreme conditions are hidden in the averaged  
17 values.

18 The CHOP method is tested in a case study where the operation of a fictive Danish combined heat and  
19 power plant is optimized over a historical 5-year period. The optimization model is solved using the full  
20 external operating condition dataset, a reduced dataset obtained using the CHOP method, a monthly-  
21 averaged dataset, a yearly-averaged dataset, and a seasonal peak/off-peak averaged dataset. The

22 economic result obtained using the CHOP-reduced dataset is significantly more accurate than that obtained  
23 using any of the other reduced datasets, while the calculation time is similar to those obtained using the  
24 monthly averaged and seasonal peak/off-peak averaged datasets. The outcomes of the study suggest that  
25 the CHOP method is advantageous compared to chronology-averaging methods in reducing external  
26 operating condition datasets to be used in the design optimization models of flexible multi-generation  
27 plants.

## 28 **Keywords**

29 Data aggregation; flexibility; multi-generation; operation optimization; polygeneration.

## 30 **Nomenclature**

### 31 **Latin letters**

32	$C$	Cost [Euro]
33	$C_v$	Power-to-heat production ratio [-]
34	$c$	Specific cost [Euro/MWh]
35	$D$	Dataset
36	$F$	Fuel consumption [MWh]
37	$N$	Number of groups
38	$n$	Number of characteristic parameter intervals
39	$O$	Operating point
40	$P$	Power [MWh]
41	$p$	Operating condition parameter
42	$Q$	Heat [MWh]
43	$T$	Time of occurrence
44	$t$	Duration [h]

### 45 **Greek letters**

46	$\alpha$	Back-pressure ratio [-]
----	----------	-------------------------

47	$\lambda$	Load [-]
48	$\sigma$	Standard deviation [-]
49	<b>Subscripts</b>	
50	<i>aa</i>	Annually averaged
51	<i>i</i>	Characteristic parameter interval index
52	<i>j</i>	Data point index
53	<i>k</i>	EOC parameter index
54	<i>l</i>	CHOP group index
55	<i>ma</i>	Monthly averaged
56	<i>pot</i>	Potential
57	<i>sp</i>	Seasonal peak/off-peak averaged

58 **Superscripts**

59	*	Linearized
----	---	------------

60 **Abbreviations**

61	CHOP	Characteristic operating pattern
62	CHP	Combined heat and power
63	EOC	External operating condition
64	FMG	Flexible multi-generation plant

65 **1. Introduction**

66 Large-scale integration of intermittent renewable energy sources (solar, wind, tidal and wave) in the energy  
67 system imposes a demand for production-consumption balancing [1]. Flexible multi-generation plants  
68 (FMGs), here defined as flexibly operating facilities integrating the production of two or more energy  
69 services (power, heating, cooling, fuels etc.), may provide such balancing operation [2]. Furthermore, FMGs  
70 based on biomass may achieve high aggregated biomass conversion efficiencies through process  
71 integration [3], which is of crucial importance in sustainable energy systems as the biomass resource is

72 limited on a global level [4] [5]. Such process integration advantages may further be used for providing  
73 sustainable fuel and energy services in FMGs at competitive prices [6] [7] [8], thereby integrating various  
74 layers of the energy system. The development of efficient biomass-processing FMGs may therefore be seen  
75 as an integral part of the transition towards a smart energy system based on renewable energy sources [9]  
76 [10].

77 The design optimization of FMG concepts includes such challenges as synthesising processes from multiple  
78 technological alternatives, facility and process dimensioning, process integration, feedstock market-impacts,  
79 operation optimization etc. In addition to this, a principal challenge is to optimize design and operational  
80 performance with respect to hourly fluctuations as well as long-term changes in demands and prices of  
81 various energy products. In principle, these data could be obtained by implementing a detailed energy  
82 system model [11] in the design optimization model, but the required data sampling, modelling, and  
83 computational effort can be prohibitive. It is therefore common to include external operating conditions  
84 (EOCs) that are hardly influenced by plant operation, such as fuel price, heating demand etc., as fixed  
85 parameters in multi-period design optimization models. In a case study of a thermal energy system,  
86 Hindsberger and Ravn [12] demonstrated that robust results can be obtained by using fixed EOC datasets  
87 when external conditions are little affected by system operation.

88 A fundamental issue in mathematical optimization models is the trade-off between level of detail and ease  
89 of solving the model. As the complexity of multi-period optimization problems increases significantly with  
90 the number of periods defined [13], it is desirable to reduce the number of period datasets without  
91 plummeting result accuracy. One approach to reducing the number of periods is to average EOC parameter  
92 values over chronological time-periods. Among averaging methods, the simplest is to average the EOCs  
93 over the lifetime of the plant (e.g. Ahmadi et al. [14], Gassner and Maréchal [15], and Chen et al. [16]). A  
94 related method is to assume annually static operating conditions, but defining each year as a period to  
95 allow for year-to-year variations caused by general energy system developments (e.g. Gerogiorgos et al.  
96 [17], and Liu et al. [18] [19]). Another method is to consider monthly average values for one key operating

97 parameter and static conditions for all other (e.g. Fazlollahi et al. [20] [21]). A more detailed approach is to  
98 consider monthly averaged EOC parameter values in a first-step optimization model, and then conduct  
99 detailed hour-wise operation optimization in a sequential step for the most promising designs (e.g. Rubio-  
100 Maya et al. [22] and Uche et al. [23]). However, neither monthly- nor annually-averaged operating  
101 parameter values provide information on short-term relations and variations between various operating  
102 conditions. While it may be acceptable to neglect this information for static operating facilities, it can be  
103 critical to the economy and thermodynamic performance of flexible facilities such as combined heat and  
104 power (CHP) plants [24] and FMGs [25] [26]. Failing to consider short-term relations between relevant  
105 operating parameters may lead to sub-optimal solutions in the design optimization of FMGs [27].  
106 One approach to reduce energy system data while maintaining details on hourly parameter relations is to  
107 represent each year by a small number of typical time-periods. Another approach is to define a number of  
108 characteristic periods, like peak-demand and off-peak-demand periods in each of the four seasons (e.g.  
109 Chen et al. [2] [28]) or typical demand days for each month based on monthly average parameter values  
110 (e.g. Mavrotas et al. [29]). These approaches rely on the assumption that operating conditions and energy  
111 demands are linked and cyclic over the seasons, an assumption that may prove inaccurate in energy  
112 systems in transition and with large shares of intermittent renewable energy production [1]. To overcome  
113 the assumption of cyclic behavior, several studies propose application of cluster analysis to identify typical  
114 periods that can be repeated in order to approximate the annual cumulative curves. Ortega et al. [30]  
115 proposed a graphical method for selecting a few typical days that can be used for representing the annual  
116 cumulative heating and cooling demand curves. Domínguez-Muñoz et al. [31] and Fazlollahi et al. [32] used  
117 a partitional clustering analysis method, the  $k$ -Medoids method, to create  $k$  typical periods. However, such  
118 approaches may hide information on peak and extreme operating conditions and lead to significant errors  
119 on peak operation performance, as also reported by Fazlollahi et al. [32] in two illustrative examples. In  
120 order to overcome these drawbacks, the duration of the typical periods may be extended to several  
121 consecutive days or even weeks (e.g. Hedegaard and Münster [33]). However, this approach increases the

122 computational effort significantly, thereby counteracting the initial ambition of reducing the number of  
123 period datasets. Instead, Bungener et al. [34] proposed a method that applied an evolutionary multi-  
124 objective optimization algorithm for identifying  $n$  sequential periods representing typical operations for an  
125 industrial cluster with the aim of minimizing standard deviation and, at the same time, maintain  
126 information on extreme operating conditions. Nemet et al. [35] presented a similar method for aggregating  
127 continuous thermal energy production and demand into sequential periods. They presented an MILP model  
128 for determining the number and duration of the periods required to obtain a certain level of accuracy over  
129 the aggregation. Karlsson et al. [36] proposed a simple method, called the TimeSlicesTool, which sorts  
130 annual operating points into three groups for critical combinations of operating characteristics and one  
131 group for all other operating points. This was done for work and non-work days in each of the four seasons,  
132 resulting in 32 groups. A drawback of this method is the fact that only information on extreme conditions is  
133 sustained, while detailed information on frequently occurring operating patterns is lost.

134 The present paper proposes a novel and simple aggregation-based method for reducing EOC datasets in  
135 optimization models. The method, named Characteristic Operating Pattern (CHOP) method, is tailored for  
136 reducing EOC datasets with non-cyclic behaviour for FMG optimization models, but it may be used for  
137 reducing similar datasets for any facility operating in multiple energy markets. In the CHOP method, EOC  
138 data points are clustered in a number of CHOP groups based on operating condition characteristics rather  
139 than on time chronology. The method thereby yields a reduction in calculation times similar to those of  
140 averaging methods ( [14] [15] [16] [17] [18] [19] [20] [21] [22] [23]) while maintaining information on short-  
141 term relations and variations between relevant operating parameters, leading to more accurate solutions.

142 Another advantage of the CHOP method is the fact that all initial EOC data are included in the reduced  
143 dataset, as opposed to typical time-period approaches ( [28] [29] [30] [31] [32] [33]) where EOC datasets  
144 are sought represented by a limited number of periods. Furthermore, the CHOP method provides a  
145 possibility for including data on long-term energy system development without *de facto* increasing the  
146 number of periods, as opposed to several of the previously described methods ( [17] [18] [19] [20] [21] [22])

147 [23], [28] [29], [34] [35] [36]). The work builds upon a preliminary study presented by Lythcke-Jørgensen et  
148 al. [27].

149 In this paper, the structure and contents of the CHOP method are described in detail in Section 2, where an  
150 example is given to demonstrate the use of the method. In Section 3, a simple operation optimization  
151 model of a CHP plant is developed, and the model is solved using various reduced EOC datasets to compare  
152 the performance of the CHOP method to other common methods. Furthermore, a posteriori error analysis  
153 is applied to assess the quality of the results obtained. In section 4 advantages and drawbacks of the CHOP  
154 method are discussed and a conclusion of the study is given in Section 5. Various reduced EOC datasets are  
155 provided in the Appendix.

## 156 **2. The Characteristic Operating Pattern method**

157 The Characteristic Operating Pattern (CHOP) method is an original graphic-based data aggregation method  
158 for reducing external operating condition (EOC) datasets. The method assumes quasi-static operation and is  
159 applicable on datasets in the form of operating points  $O_j$ , with each point being characterised by a time of  
160 occurrence  $T_j$ , a duration  $t_j^1$ , and a number of operating condition parameters  $\bar{p}_j$ .

$$161 \quad O_j = \{T_j, t_j, \bar{p}_j\} \quad (1)$$

162 In the CHOP method, EOC data points are clustered in groups based on data characteristics rather than the  
163 time of occurrence, as opposed to time-chronological averaging methods [ [14] [15] [16] [17] [18] [19] [20]  
164 [21] [22] [23]]. The clustered groups, called CHOP groups, are introduced as weighted periods in multi-  
165 period optimization models. A principal sketch of the data aggregation principle applied in the CHOP  
166 method is presented in Figure 1. Dynamics cannot be considered in operation optimization models applying  
167 CHOP-reduced datasets as information on time chronology is lost.

168 Two overall procedures are associated with the CHOP method: The CHOP data aggregation method, and  
169 error analysis. The CHOP data aggregation method, which is the core of the method, consists of three  
170 principal steps:

---

<sup>1</sup>  $t_{O_j} = 1h$  is commonly used when working with power markets [37], but other values of  $t_j$  may be used as well.



- 171 1. *Entity selection*: Identification of relevant EOC parameters
- 172 2. *Clustering criteria*: Definition of characteristic parameter intervals
- 173 3. *Cluster procedure*: Establishment of CHOP groups

174 As it is desirable to estimate the quality of the results obtained using the reduced dataset, error analysis is  
175 an integral part of the CHOP method. Within the framework presented here, one *a priori* and two *a*  
176 *posteriori* analyses are suggested, but others may be relevant as well.

- 177 1. *A priori*: Evaluate the standard deviation of parameters in CHOP groups
- 178 2. *A posteriori*: Evaluate the quality of the applied datapoint clustering. Analyse the errors made by  
179 neglecting dynamic constraints.

180 Both *a priori* and *a posteriori* error analyses may yield results necessitating reconfiguration of the data  
181 aggregation analysis. The overall CHOP method procedure is illustrated in Figure 2.

182 Next, the contents of the CHOP data aggregation analysis and suggestions for error analyses are presented.

183 The method is illustrated by an *example*, in which a historical 5-year EOC dataset for a fictive local  
184 extraction-based combined heat and power (CHP) plant located in West Denmark is reduced using the  
185 method. A principal sketch of the CHP plant is shown in Figure 3.

## 186 2.1. CHOP data aggregation method

### 187 2.1.1. Entity selection

188 The first step in the CHOP data aggregation analysis is to select data entities for clustering. This implies 1)  
189 identification of EOC parameters  $p_k$  for the plant of interest, and 2) assessment of parameter variation:

- 190 1) **Identification of relevant EOC Parameters**: Within the CHOP method framework, EOCs are defined  
191 as boundary conditions that may influence, but are hardly influenced by, operation decisions on  
192 plant level, and are therefore regarded as fixed parameters. Any parameter fitting these criteria  
193 must be included as an EOC parameter.
- 194 2) **Parameter variation assessment**: For all identified EOC parameters, the maximum, minimum and  
195 mean parameter values over the selected period must be identified based on the reference

196 datasets. As it is desirable to reduce the number of EOC parameters to define clustering from in  
197 order to keep computational effort low, it is recommended that clustering criteria are only defined  
198 for EOC parameters with variations higher than  $\pm 10\%$  of the period mean value. The potential  
199 error from neglecting variations in specific EOC parameters must be assessed as a part of the  
200 *posteriori* error analysis, see section 2.2.2.

201 *Example:* As illustrated in Figure 3, the CHP plant of interest imports fuel, air, and cooling water, while it  
202 produces district heating, power, exhaust gases and heated cooling water.

### 203 **1) Identification of the relevant EOC parameters**

204 The assumed objective of the CHP plant owner is to obtain the most profitable production. Being the sole  
205 heat producer in the district heating system, the production of a CHP plant is constrained by the heating  
206 demand. Assuming that cooling is freely available from a cold reservoir, air is freely available from the  
207 surroundings, and neglecting taxes on emissions, three relevant EOC parameters exist: Fuel price (coal),  
208 heating demand, and power price. Being a single plant located in the well-integrated West Denmark power  
209 grid, the power and coal prices can be considered unaffected by the production of the CHP plant. Assuming  
210 no demand flexibility on the consumer side, the heat demand is also unaffected by operation decisions.  
211 Hence, these three external parameters can be considered as EOC parameters in the CHOP method. This  
212 would not have been the case had the CHP plant been the main power producer in an isolated power grid,  
213 or if the CHP plant was fuelled by a local distributed biomass like straw [38], in which case the power  
214 and/or fuel prices would have been significantly influenced by plant operation decisions.

### 215 **2) Assessment of parameter variation**

216 Historical parameter datasets over the period 2010-01-01 – 2014-12-31 are considered for the three EOC  
217 parameters.

218 According to data on coal prices from Key World Energy Statistics 2014 provided by the International  
219 Energy Agency [39], the yearly average coal price in Denmark's neighbouring country Poland was 80.75  
220 USD/ton over the years 2010-2013, with a maximum price of 84 USD/ton and a minimum price of 78

221 USD/ton. Assuming that the coal price fluctuations in Poland are analogue to those in Denmark, the  
222 resulting variation range is -3.4% to +4% which is well below the recommended clustering threshold of  
223  $\pm 10\%$ . Therefore, the coal price is not considered as a varying EOC parameter for clustering in the case  
224 treated. The error of this assumption will be assessed as a part of the *posteriori* error analysis in Section 3.4.  
225 In the given case, the coal price is set to 15.70 Euro/MWh, which is the perceived coal price for 2012  
226 reported by the Danish CHP owner DONG Energy [40].

227 Data on hourly power prices in West Denmark over the entire period has been extracted from the webpage  
228 of the Danish transmission system operator Energinet.dk. [41]. The average hourly power price was 40.08  
229 Euro/MWh, with a maximum price of 2000.00 Euro/MWh and a minimum price of -200.00 Euro/MWh. As  
230 this variation is well above the recommended threshold of  $\pm 10\%$  of the mean, power price is included as a  
231 varying EOC parameter for clustering.

232 Data on hourly relative heat demand in a Danish district heating system over a year has been extracted  
233 from the energy system model STREAM [42]. It is assumed that the annual relative heat demand pattern is  
234 repeated for each of the 5 years investigated. The average hourly relative heat demand over the period was  
235 0.55, with a maximum of 1.00 and a minimum of 0.06. As this gives in a variation of -89% to +82% which  
236 is well above the recommended threshold of  $\pm 10\%$  of the mean, relative heat demand is included as a  
237 varying EOC parameter for clustering.

### 238 2.1.2. Clustering criteria

239 Having identified the varying EOC parameters  $p_k$ , the second step of the CHOP data aggregation analysis is  
240 to define the clustering criteria for aggregating operating points. This is done by splitting the value range of  
241 each  $p_k$  into a number of characteristic intervals,  $n_{p_k}$ . Being empirical in essence, the following graphic-  
242 based two-step approach is suggested for breaking up a parameter value range into characteristic intervals  
243 based on the cumulative parameter curve. The process is illustrated in Figure 4 with power price as the  
244 relevant EOC parameter.

- 245 a) **Important values:** Some parameter values may be of special interest, making it relevant to  
246 introduce a break at these points. For the power price example, it may be relevant to introduce a  
247 break at a power price of 0.00 Euro/MWh to make sure that negative prices are grouped together.  
248 Also, if an operating decision, e.g. turning on a piece of equipment, is dependent on a given power  
249 price, an interval break should be introduced at this price as well. It is also suggested that if  
250 significant trend changes occur in the cumulative curve, the parameter values of points separating  
251 various trends should be included as important values.
- 252 b) **Even division:** If the already set break-points are far from each other in terms of both parameter  
253 value and duration, it is suggested that additional interval breaks are introduced to minimize the  
254 span. The break-points should be located so that the parameter value range is constant for each of  
255 the intervals.

256 It is essential that all feasible parameter values are covered within the characteristic parameter intervals. It  
257 may be necessary to define the first and last of the characteristic intervals as open. The necessary number  
258 of intervals for each parameter depends on the parameter value volatility, the significance of the  
259 parameter and the data available. In Figure 4, six intervals were defined in the visual power price example,  
260 while it may be sufficient to define just two or three intervals for less volatile parameters. In contrast, more  
261 intervals may be defined for the power price in case it has significant impact on the optimization model. It  
262 should be noticed that if only one characteristic interval is defined for a parameter, it will be included as a  
263 constant in the final CHOP-reduced dataset.

264 *Example:* The cumulative curve for power prices, also known as the power price duration curve, is obtained  
265 by sorting the data points according to the value of the power price value. The cumulative curve illustrates  
266 the aggregated duration of power prices over the period, and is shown in Figure 5.

267 Using the suggested two-step approach for breaking up the cumulative curve for power prices, the  
268 following break points are obtained:

- 269 a) Important values: 0.00, 25.00, 65.00 [Euro/MWh]

270 b) Even division: 35.00, 45.00, 55.00 [Euro/MWh]

271 This leads to seven characteristic intervals for the power price, which are summarized in Table 1.

272 The cumulative curve for the relative heat demand, which illustrates the aggregated duration of relative  
273 heat loads over the period, is shown in Figure 6.

274 Using the suggested two-step approach for breaking up the cumulative curve for relative heat demand, the  
275 following break points are obtained:

276 a) Important values: 0.25, 0.65, 0.95<sup>b</sup> [-]

277 b) Even division: 0.125, 0.45, 0.80 [-]

278 <sup>b</sup> It is relevant to group peak heat-demand operating points together for heat production dimensioning purposes.

279 This leads to seven characteristic intervals for the relative heat demand, which are summarized in Table 2.

### 280 2.1.3. Cluster procedure

281 The final part of the data aggregation analysis is the cluster procedure, which involves the definition of  
282 CHOP groups and clustering and aggregation of data points in the CHOP groups.

283 By definition, any combination of characteristic parameter intervals is a potential CHOP group. Hence, the  
284 number of potential CHOP groups in a dataset,  $N_{CHOP,pot}$ , is determined by the number of characteristic  
285 parameter intervals  $n_{p_k}$  defined for each of the varying EOC parameters  $p_k$ :

$$286 \quad N_{CHOP,pot} = \prod_{p_k} n_{p_k} \quad (2)$$

287 To maintain an overview, it is suggested that the potential CHOP groups are indexed using the following  
288 key:

$$289 \quad G_l = G(i_{p_1}, i_{p_2}, \dots, i_{p_k}) \quad (3)$$

290 Here,  $G$  is short for group, and  $i_{p_n} \in \{1, \dots, n_{p_k}\}$  is the interval number  $i$  of the varying EOC parameter  $p_k$ .

291 For example, if two varying EOC parameters are defined in a CHOP-reduced dataset, the CHOP group

292  $G(2,5)$  represents the combination of ' $p_1$  interval 2' and ' $p_2$  interval 5'. EOC parameters considered as

293 constants are not included in the indexing key.

294 All data points  $O_j$  of the initial dataset are sorted into the potential CHOP groups  $G_l$  based on their EOC  
 295 parameter values. Each CHOP group  $G_l$  becomes an operating point in the final dataset characterised by a  
 296 duration  $t_l$  (the sum of durations of the aggregated data points), and a number of operating condition  
 297 parameters  $\bar{p}_l$  (the weighted average parameter values of the aggregated data points).

$$298 \quad G(i_{p_1}, i_{p_2}, \dots, i_{p_k}) = G_l = \{t_l, \bar{p}_l\} \quad (4)$$

$$299 \quad t_l = \sum_{O_j \in G_l} t_j \quad (5)$$

$$300 \quad \bar{p}_l = \frac{\sum_{O_j \in G_l} \bar{p}_j \cdot t_j}{t_l} \quad (6)$$

301 It should be noted that the vector  $\bar{p}_l$  includes all EOC parameters, but it may also include other external  
 302 parameters that are unaffected by the plant operation. It is evident that the duration  $t_j$  represents the  
 303 weight given to a given operating point  $O_j$  in the CHOP dataset. In case the time-value of money is  
 304 considered in the optimization model,  $t_j$  can be represented in the form of present value factor  $t_{PV,j}$  as  
 305 well.

306 If no data points belong to a potential CHOP group, the group is excluded from the final CHOP dataset.

307 Hence, the final number of CHOP groups is lower than or equal to the number of potential CHOP groups:

$$308 \quad N_{CHOP} \leq N_{CHOP,pot} = \prod_{p_k} n_{p_k} \quad (7)$$

309 The defined CHOP groups  $G_l$  replace the initial dataset of operating points in an optimization model,  
 310 thereby reducing the number of periods to be considered.

311 *Example:* Three EOC parameters are considered: Relative heat demand  $p_1$ , power price  $p_2$ , and coal price  
 312  $p_3$ . The number of characteristic parameter intervals are  $n_{p_1} = 7$ ,  $n_{p_2} = 7$ , and  $n_{p_3} = 1$ . Hence, the  
 313 number of potential CHOP groups  $N_{CHOP,pot}$  is

$$314 \quad N_{CHOP,pot} = \prod_{p_k} n_{p_k} = 49 \quad (8)$$

315 Based on the reference dataset, a simple algorithm written in Excel was applied for sorting reference data  
 316 points into CHOP groups. Using equations (4)-(6), the algorithm further calculated durations and parameter  
 317 values for the identified CHOP groups. The processing of the entire dataset took approximately 30 seconds

318 using a laptop with an Intel® Core™ i7-3720QM CPU with 2.60 GHz and 8 GB RAM. The calculated values  
319 are summarized in Table 3.

320 The number of CHOP groups is found to be

$$321 \quad N_{CHOP} = 46 < N_{CHOP,pot} \quad (9)$$

322 as no data points belongs to the potential CHOP groups  $G(1,1)$ ,  $G(1,7)$  and  $G(7,1)$ . An illustration of the  
323 sorting of data points into CHOP groups and the resulting CHOP groups is presented in Figure 7.

## 324 **2.2. Error analysis**

### 325 **2.2.1. A priori**

326 Having conducted the data aggregation analysis, it is possible *a priori* to calculate the standard deviation  
327  $\sigma_{p_{k,l}}$  for each parameter  $p_k$  in a CHOP group  $G_l$ .

$$328 \quad \sigma_{p_{k,l}} = \sqrt{\frac{1}{t_l} \sum_j (t_j (p_{k,j} - p_{k,l})^2)} \quad (10)$$

329 with  $t_j$  being the duration of an operating point  $O_j \in G_l$  and  $t_l$  being the summarized duration of  $G_l$ . The  
330 standard deviation may give an impression of the scatter of the merged operating points within each CHOP  
331 group and thereby estimate the accuracy error of aggregating numbers in the defined CHOP groups. If the  
332 standard deviation of a parameter is significantly larger in one CHOP group than in the others, the cause of  
333 the deviation should be investigated. Significant standard deviations may indicate that additional  
334 characteristic intervals have to be defined in the CHOP data aggregation analysis.

335 *Example:* The standard deviation is calculated for the relative heat demand and power price of the CHOP  
336 groups defined in Table 3. The results are presented in Table 4 and Table 5.

337 Concerning the standard deviation of the relative heat demand, it is seen that the largest deviations occur  
338 for the heat intervals 3 and 4, owing to the fact that these two intervals are the ones with the largest value  
339 span. The standard deviations are not found to vary significantly, and it is therefore not considered  
340 necessary to change the characteristic intervals for the relative heat demand.

341 Regarding the standard deviation of the power price, significant differences are obtained for power price  
342 intervals 1 and 7. The reason is that the intervals contain extreme parameter values as they are open  
343 towards the infinite. Especially groups  $G(5,1)$  and  $G(4,7)$  show large standard deviations, which is also  
344 evident from Figure 7. For  $G(5,1)$ , the major deviation is caused by 8 hours on the December 25<sup>th</sup> 2012  
345 when the average power price was -174.87 Euro/MWh. For  $G(4,7)$ , the main cause of the large deviation is  
346 5 hours on June 7<sup>th</sup> 2013 when the average power price was 1940.82 Euro/MWh. Based on these findings, it  
347 is not deemed relevant to change the characteristic intervals *a priori*.

### 348 2.2.2. A posteriori error analysis

349 Having solved an optimization model using CHOP-reduced datasets, two suggestions for *a posteriori*  
350 analyses are presented here: A sensitivity analysis for verifying the quality of the CHOP-groups and  
351 selection of varying EOC parameters, and an error analysis for estimating errors from neglecting time  
352 chronology-dependent constraints, such as production ramp rates or thermal storages.

353 To verify the quality of the CHOP-group clustering criteria, new CHOP datasets can be defined from the  
354 initial EOC dataset but with additional characteristic intervals for each parameter. New operation  
355 optimization runs can then be made for selected designs using the new CHOP group datasets. If results of  
356 the various runs differ significantly, it may suggest that the characteristic intervals have been defined too  
357 loosely and that a more detailed CHOP data aggregation should be conducted for the dataset.

358 *Example:* An example of how to evaluate the CHOP group clustering criteria using sensitivity analysis, and  
359 to assess the expected error of including an EOC parameter as a constant, is given in Section 3.4.

360 Some optimization models may include constraints that require knowledge on time chronology, for  
361 instance ramp-rate or thermal storage constraints. However, this information is not sustained in CHOP-  
362 reduced datasets. If an optimization model with time chronology-dependent constraints is run using CHOP-  
363 reduced EOC datasets, the error of neglecting these constraints must be assessed *a posteriori*. This can be  
364 done by first solving the optimization model using the CHOP-reduced EOC dataset. The found optimal



365 operation pattern can then be applied on the initial EOC dataset, and the resulting error of neglecting the  
366 constraint can be calculated.

367 *Example:* An example of how to assess the error of including a thermal storage in an optimization model  
368 using a CHOP-reduced EOC dataset is presented in Section 3.5.

### 369 **3. Illustrative case: Operation optimization of a Danish extraction-based** 370 **combined heat and power plant**

371 In this section, the advantage of applying the CHOP method is illustrated by extending the CHP-example of  
372 section 2. Here, the operation of the fictive Danish extraction-based CHP is optimized over the 5-year  
373 period 2010-01-01 – 2014-12-31. The optimization is carried out using the entire EOC dataset, the CHOP-  
374 reduced dataset, a yearly averaged dataset, a monthly averaged dataset, and a seasonal peak/off-peak  
375 averaged dataset. The results obtained are compared with respect to problem size and accuracy.

#### 376 **3.1. Optimization model**

377 A linearized model of the existing Danish extraction-based CHP plant Avedøreværket 1 (AVV1) is developed  
378 to represent the fictive Danish CHP plant treated in the example. AVV1 was commissioned in 1990 and has  
379 a net power production of 250 MW in condensation mode and 212 MW in full back pressure mode with a  
380 district heating production of 330 MJ/s (drive temperature/return temperature 100°C/50°C) [43]. Part-load  
381 operation in the CHP unit is governed by sliding-pressure control [44]. The minimum load  $\lambda_{min}$  considered  
382 of AVV1 is  $\lambda_{min} = 0.4$ .

383 A thermodynamic model of AVV1 was previously developed by Elmegaard and Houbak [43] using the  
384 energy system simulator Dynamic Network Analysis [45]. The model was validated by Lythcke-Jørgensen et  
385 al. [25], who found that the model-predicted electrical efficiency in condensation mode was 2%-8% lower  
386 than that reported by the plant owner, but that the model in general was accurate with respect to electrical  
387 and first-law energy efficiency. The linearized model developed here is based on the model by Elmegaard  
388 and Houbak [43].

389 The linearized model is based on two assumptions: The power-to-heat production ratio  $C_v$  is constant, and  
 390 the fuel-consumption is a linear function of the load. Four central operating points in the reference model  
 391 {A, B, C, D} are used for developing the linearized model: A is operation in full-load condensation-mode, B is  
 392 operation in minimum-load condensation-mode, C is operation in full-load back-pressure-mode, and D is  
 393 operation in minimum-load back-pressure-mode.

394 In the linear model, the linearized operating points A\* and C\* are set equal to the reference points A and C,  
 395 while heat production in the linearized points B\* and D\* is set equal to the heat production of reference  
 396 points B and D.

$$397 \quad A^* = A \quad , \quad C^* = C \quad , \quad Q_B^* = Q_B \quad , \quad Q_D^* = Q_D \quad (11)$$

398 The linearized power-to-heat ratio  $C_v^*$  is defined as the average of the overall heat-to-power ratios at  
 399 maximum load,  $C_{v,\lambda_{max}}$ , and minimum load  $C_{v,\lambda_{min}}$ :

$$400 \quad C_{v,\lambda_{max}} = \frac{Q_B}{P_A - P_B} \quad (12)$$

$$401 \quad C_{v,\lambda_{min}} = \frac{Q_D}{P_C - P_D} \quad (13)$$

$$402 \quad C_v^* = \frac{C_{v,\lambda_{max}} + C_{v,\lambda_{min}}}{2} = 9.406 \quad (14)$$

403 The power production in the linearized points B\* and D\* are found using equations (11) and (14). Data on  
 404 the four reference points {A, B, C, D} and the corresponding linearized points {A\*, B\*, C\*, D\*} are presented  
 405 in Table 6.

406 For any heat production  $Q$ , the maximum power production in the linearized model  $P_{max}^*$ , which  
 407 corresponds to a power production at a load  $\lambda = 1.0$ , is

$$408 \quad P_{max}^* = P_A^* - \frac{Q}{C_v^*} \quad (15)$$

409 Two constraints exist on the minimum power production in the linearized model,  $P_{min1}^*$  and  $P_{min2}^* \cdot P_{min1}^*$   
 410 is the minimum feasible power production as a consequence of the minimum load constraint  $\lambda_{min} = 0.4$  ,  
 411 while  $P_{min2}^*$  is the minimum feasible power production as a consequence of the back-pressure operation-  
 412 mode constraint  $\alpha_{max} = 1.0$ . Both of these constraints must be satisfied.

413 
$$P_{min1}^* = P_C^* - \frac{Q}{C_v^*} \quad (16)$$

414 
$$P_{min2} = P_D^* + (Q - Q_D^*) \frac{P_B^* - P_D^*}{Q_B^* - Q_D^*} \quad (17)$$

415 The feasible power-heat operation area of the linearized model is defined by the constraints (15)-(17). The  
 416 power-heat operation area of the reference model, the linearized model, and the four reference operating  
 417 points {A, B, C, D} are shown in Figure 8.

418 Evaluating the accuracy of the linear approximated equations (15)-(17), it is found that the accuracy on the  
 419 power constraints is within -1.45% to 2.69%. The largest negative deviation occurs for the maximum power  
 420 production at  $Q = 194.5 \text{ MJ/s}$ , and the largest positive deviation occurs for the minimum power  
 421 production at  $Q = 118.6 \text{ MJ/s}$ .

422 In the linearized model, the load can be calculated as a function of the heat and power production:

423 
$$\lambda(P, Q) = \lambda_{min} + (1 - \lambda_{min}) \frac{\left(\frac{P+Q}{C_v^*}\right) - P_C^*}{P_A^* - P_C^*} \quad (18)$$

424 The linearized fuel consumption  $F^*(\lambda)$  in MJ/s as a function of the load is found using the first-order  
 425 trendline function in Microsoft Excel on data for fuel consumption at various loads in the AVV1 model.

426 
$$F^*(\lambda) = F^*(P, Q) = 499.64 \cdot \lambda(P, Q) + 102.179 \quad (19)$$

427 A coefficient of determination of  $R^2 = 0.9998$  was obtained for this trendline function.

428 The operation of the fictive Danish CHP plant is to be optimized with the aim of minimizing the costs of  
 429 producing heat to the district heating network over the period 2010-01-01 – 2014-12-31. The variables of  
 430 the optimization model are the power production  $P_j$  and heat production  $Q_j$  in each period  $j$ . As discussed  
 431 in Section 2.1., the CHP production is constrained by the heating demand which has to be met at all times.

432 *To simplify matters, thermal energy storage is neglected, hence  $Q_j$  is constrained by*

433 
$$Q_j = Q_{j,ref} \quad \forall j \quad (20)$$

434 The power production  $P_j$  is constrained by equations (15)-(17). *Full hour-wise operation flexibility is*  
 435 *assumed for the plant, and, consequently, the choice of  $(P_{j+1}, Q_{j+1})$  is independent of  $(P_j, Q_j)$ .*

436 Assuming that operation and maintenance costs are constant and therefore indifferent to the choice of  
 437  $(Q_j, P_j)$ , that air is free and cooling is freely available from a cold reservoir, and neglecting taxes on  
 438 emissions, the objective function to be minimized can be defined as

$$439 \quad C_{heat}(Q_j, P_j) = \sum_j [F^*(P_j, Q_j) \cdot c_{fuel,j} - P_j \cdot c_{p,j}] \quad (21)$$

440 Here,  $C_{heat}(Q_j, P_j)$  is the variable cost of the heat production,  $c_{fuel,j}$  is the cost of fuel, and  $c_{p,j}$  is the  
 441 power price in each operating point  $j$ .

442 Given equations (15)-(21), the optimization problem can be written in condensed form as

$$443 \quad \begin{cases} \min_{Q,P} [C_{heat}(Q_j, P_j)] \\ \text{subject to constraints:} \\ \text{equations (15), (16), (17), (20)} \\ \text{with variables:} \\ P_j, Q_j \in \mathbb{R}^+ \end{cases} \quad (22)$$

### 444 3.2. External operating conditions datasets

445 Five different EOC datasets are used for solving optimization problem (22): The full EOC dataset, which is  
 446 obtained by combining data on hourly power prices in the West Denmark power grid [41] with data on  
 447 hourly relative heat demand for Denmark [42], as discussed in Section 2.1.2; the CHOP-reduced EOC  
 448 dataset  $D_{CHOP}$ , which is presented in Table 3; the annually averaged EOC dataset  $D_{AA}$ , in which the EOC  
 449 parameter values are averaged over each of the five years; the monthly averaged EOC dataset  $D_{MA}$ , in  
 450 which the EOC parameter values are averaged over each of the 60 months in the period; and, finally, the  
 451 seasonal peak/off-peak averaged EOC dataset  $D_{SP}$ , which is inspired by the approach taken by Chen et al.  
 452 [2] for representing EOC parameters. Here, EOC parameter values are averaged over the peak period, 7  
 453 a.m.-11 p.m., and off-peak period, 11 p.m.-7 a.m., for each of the four seasons each year. Datasets  $D_{AA}$ ,  
 454  $D_{MA}$ , and  $D_{SP}$  are presented in the Appendix. A scatter diagram illustrating the reference EOC dataset and  
 455 the reduced datasets is presented in Figure 9.

456 Figure 9 illustrates how the parameter value diversity of the reference dataset is sustained in the various  
 457 reduced datasets. It is seen that the annual average EOC dataset yields five points, all located in the centre  
 458 of Figure 9, that are almost identical with respect to relative heat demand and power price. The monthly

459 averaged and seasonal peak/off-peak averaged EOC datasets are seen to be more distributed, but the  
460 resulting operating points are still far from the borders of the dense cloud of reference operating points.  
461 Opposed to this, both the CHOP and the CHOP-revised EOC datasets are seen to be significantly more  
462 distributed in the figure, suggesting that a larger degree of the diversity in the reference dataset is  
463 sustained in these reduced datasets.

### 464 **3.3. Results and comparison**

465 The optimization problem (21) is solved using the open-source mixed-integer program solver CBC (COIN  
466 Branch and Cut) [46] in OpenSolver 2.6.1 [47] for Microsoft Excel. The optimization results obtained using  
467 each of the five EOC datasets are summarized in Table 7.

468 Firstly, it is evident that by optimizing the operation of the CHP unit using the full dataset it is possible to  
469 reduce the total variable heat cost to  $C_{heat} = 0.38$  MEuro. This value is the exact solution to the  
470 optimization problem (21) under the given conditions and assumptions, and the results obtained using the  
471 full dataset are used as reference values for further comparison.

472 Among the reduced EOC datasets, the result obtained using  $D_{CHOP}$  gets closest to the reference value with  
473 a deviation of 0.38 MEuro in total variable heat cost. Compared to this, the deviation is 8.15 MEuro when  
474 using  $D_{AA}$ , 7.64 MEuro using  $D_{MA}$ , and 5.58 MEuro using  $D_{SP}$ . In terms of computation time, the number of  
475 calculations to be performed is 5 when using  $D_{AA}$ , 60 when using  $D_{MA}$ , 40 when using  $D_{SP}$ , and 46 when  
476 using  $D_{CHOP}$ . Hence,  $D_{CHOP}$  obtains the most accurate economic result of the reduced datasets for the case,  
477 while the relative reduction in computation time from using  $D_{CHOP}$  is comparable to those of using  $D_{MA}$   
478 and  $D_{SP}$ . This demonstrates the relevance of the CHOP method for reducing datasets on external operating  
479 conditions.

480 For the results obtained using  $D_{AA}$ ,  $D_{MA}$  and  $D_{SP}$ , it is seen that the total power production and fuel  
481 consumption are larger than the reference values. This is caused by the fact that the operation optimization  
482 only considers the average power prices of the periods. Hence, if the average power price over a given  
483 period is economically attractive for power production at the plant, power production is maximized over

484 the entire period even though the power price may not be attractive in all hours. This phenomenon results  
485 in an increased power production, but also in increased fuel costs that exceed the increased income from  
486 power sales and yielding a higher  $C_{heat}$  for the three solutions compared to the reference solution. The  
487 opposite trend, where power production is minimized for entire periods containing data points with  
488 advantageous power prices, also occurs when using  $D_{AA}$ ,  $D_{MA}$  and  $D_{SP}$ , but the first trend is found to be  
489 dominant in the present case.

490 In contrast, the result obtained using the  $D_{CHOP}$  dataset underestimates the power production in the case  
491 investigated, and also shows reduced income from power sales. At the same time an almost equal  
492 reduction in fuel costs occurs, resulting in the relatively low deviation in the heat price compared to the  
493 reference result. The explanation is that in the CHOP method, the data points merged in CHOP groups have  
494 similar parameter values. Hence, averaged parameter values are close to the parameter values of the data  
495 points. If the power is minimized over a data point where it would be maximized in the reference case, or  
496 vice versa, the economic difference is small. Thus, when using the  $D_{CHOP}$  dataset, the economic result is  
497 very close to that of the reference optimization.

498 Comparing the accuracy of results, it is seen that the estimated fuel consumption and power production  
499 are overestimated by 2.5% and 3.4% using  $D_{AA}$ , by 4.4% and 5.7% using  $D_{MA}$ , by 2.2% and 2.8% using  $D_{SP}$ ,  
500 while they are underestimated by 3.1% and 4.1% using  $D_{CHOP}$ . This indicates that the optimal operation  
501 pattern predicted using  $D_{CHOP}$  is different from the reference optimum for a significant amount of  
502 operating points for the given case, suggesting that the CHOP clustering criteria could be improved. This  
503 had not been obvious if the reference solution had not been known, or if only the economic objective had  
504 been considered. Therefore, it is suggested that sensitivity analysis is applied *a posteriori* for evaluating the  
505 quality of the applied clustering criteria, and thereby assessing the accuracy of the results.

### 506 **3.4. Sensitivity analysis**

507 *A posteriori*, sensitivity analyses are conducted to evaluate the quality of the entity selection and the  
508 applied clustering criteria.

509 First, the impact of not including coal price as a varying EOC parameter in the CHOP analysis is assessed. As  
510 described in Section 2.1.1., the data suggested that the coal price varied within the range -3.4% to +4% of  
511 the average price over the period. It is here assessed how such variations would affect the optimized  
512 operating pattern when using the CHOP dataset.

513 In the optimization model, the heat production is constrained and therefore unaffected by the coal price.  
514 However, power production is flexible and depends on power prices and coal prices. The impact on power  
515 production and fuel consumption from varying the coal price within the range  $\pm 5\%$  over the entire period  
516 is shown in Figure 10. It is seen that if the coal price is reduced by 5%, the power production is increased by  
517 1.2% and the fuel consumption by 0.9%. Apart from this, the power production and fuel consumption are  
518 hardly affected by variations in the coal price over the set range. It is therefore considered acceptable to  
519 use the average coal price value in the CHOP dataset.

520 Next, the applied clustering criteria are assessed. Here, the number of characteristic intervals defined for  
521 the relative heat demand and power price is varied and new CHOP datasets are obtained. The optimization  
522 model is then run using each of the new CHOP datasets to evaluate the impact on the results of changing  
523 the clustering criteria.

524 Three sensitivity analyses are considered: Heat interval sensitivity, where the number of intervals defined  
525 for the relative heat demand is changed; power interval sensitivity, where the number of intervals defined  
526 for the power price is changed; and combined heat and power interval sensitivity, where the number of  
527 intervals defined for both the relative heat demand and the power price are changed simultaneously. The  
528 interval break points defined for the sensitivity analyses are given in Table 8.

529 The results obtained by running the optimization model with the modified CHOP datasets are compared  
530 with respect to income result, fuel cost, power production and power sales. The outcomes are presented in  
531 Figures 11-14.

532 Figure 11 shows the variations in total variable heat cost from the different sensitivity analyses. It is seen  
533 that *reducing the number of power intervals with the suggested break-points significantly increases the*

534 *total variable heat cost*, while increasing the number of intervals leads to slightly better results. A stable  
535 level is reached when increasing the number of power price intervals to 8-10 with the set break points. This  
536 suggests that the number of characteristic intervals for the power price should be increased in order to  
537 obtain a robust solution. Opposed to this, *the result is almost unaffected by the number of relative heat*  
538 *demand intervals defined*, suggesting that the initial resolution of 7 characteristic heat demand intervals is  
539 sufficient. Both findings are supported by the combined heat and power intervals sensitivity analysis, the  
540 trend of which is almost identical to that of the power interval sensitivity.

541 Furthermore, the findings above are supported by the analogue results obtained when comparing the  
542 sensitivity analysis results with respect to fuel costs (Figure 12), power production (Figure 13), and power  
543 sales (Figure 14). Again, it is found that the results are somewhat unaffected by minor changes in the  
544 number of relative heat demand characteristic intervals, while the results obtained become stable when  
545 the number of power price intervals is increased to 8 or more using the suggested interval break-points.

546 The sensitivity analysis suggests that the CHOP dataset should be reconfigured by changing the number of  
547 characteristic power price intervals to 8 using the interval break-points presented in Table 8. The revised  
548 CHOP dataset is presented in Table 9, while results obtained using the revised CHOP dataset are presented  
549 in Table 10. The results show that the  $C_{heat}$  obtained is practically identical to that found using the  
550 reference data when applying the revised CHOP dataset, while the power production and fuel consumption  
551 are underestimated by less than 1%, suggesting that the revised clustering criteria is more accurate than  
552 the initial one. In terms of reduction in relative computation time, the revised CHOP dataset requires 53  
553 calculations, a number which is comparable to the number of calculations required when using  $D_{MA}$  and  
554  $D_{SP}$  as well.

### 555 **3.5. Optimization with thermal energy storage**

556 As discussed by Rolfsman [48], the income from power sales in CHP plants may be increased by installing  
557 thermal energy storages that allows for production shifting in periods with high power prices. Similar  
558 results were reported by Martínéz-Lear et al. [49] for combined heating, cooling and power plants for



559 buildings. Hence, optimization models of multi-generation plants dealing with heating or cooling  
 560 production should preferably include an option for thermal storage. In this section, the optimization model  
 561 (22) is rewritten to include short-term heat storage, and the error made from solving the problem using the  
 562 revised CHOP dataset (Table 9) is assessed.

563 In the case of the fictive Danish CHP plant, it is assumed that a thermal energy storage capable of storing 24  
 564 hours of peak heat production is available on site.

$$565 \quad Q_{storage,max} = 24 \cdot 332.91 MWh = 7990 MWh \quad (23)$$

566 Heat losses are neglected in the thermal energy storage model. The thermal energy storage content

567  $Q_{storage,j}$  is calculated as

$$568 \quad Q_{storage,j} = Q_{storage,j-1} + (Q_j - Q_{j,ref}) \quad , \quad Q_{storage,0} = 0 \quad (24)$$

569 In the rewritten optimization problem, the constraint (19) is slacked and replaced by a new constraint  
 570 stating that the total heat production over the entire period must equal the total heat consumption

$$571 \quad \sum_j Q_j = \sum_j Q_{j,ref} \quad (25)$$

572 Furthermore, two constraints are introduced representing the physical constraints of the thermal energy  
 573 storage:

$$574 \quad Q_{storage,j} \leq Q_{storage,max} \quad (26)$$

$$575 \quad Q_{storage,j} \geq 0 \quad (27)$$

576 Given equations (15)-(19) and (23)-(27), the optimization problem with thermal energy storage can be  
 577 written in condensed form as

$$578 \quad \begin{cases} \min_{Q,P} [C_{heat}(Q_j, P_j)] \\ \text{subject to constraints:} \\ \text{equations (15), (16), (17), (25), (26), (27)} \\ \text{with variables:} \\ P_j, Q_j \in \mathbb{R}^+ \end{cases} \quad (28)$$

579 As constraints (26) and (27) require knowledge of the time chronology of the data points, the optimization  
 580 problem (28) cannot be solved using the CHOP-reduced dataset. Therefore, constraints (26) and (27) were

581 slacked, and the resulting error was evaluated a posteriori. Results obtained from solving the problem (28)  
582 using the full EOC dataset and the revised CHOP dataset are presented in Table 11.

583 When solving problem (28) using the full EOC dataset, a total variable heat cost of -6.08 MEuro was  
584 obtained, as opposed to the solution where no heat storage was considered and a total variable heat cost  
585 of 0.38 MEuro was obtained. The negative costs means that power sales exceed the total fuel costs in  
586 optimal operation for the CHP plant. The result suggests that short-term thermal energy storage is an  
587 economic advantage in CHP production, supporting the outcomes presented by Rolfsman [48] and  
588 Martínéz-Lear et al. [49]. It is further seen that the power production is slightly reduced while incomes from  
589 power sales are increased when comparing to the situation without heat storage. This is owing to the fact  
590 that heat storage allows for a more flexible production.

591 Solving problem (28) with the revised CHOP dataset gives a total variable heat cost of -8.06 MEuro. It is  
592 seen that the power production, power sales, and fuel consumption are all reduced when compared to the  
593 solution obtained using the full EOC dataset. The economic result is slightly improved when compared to  
594 the result obtained using the full EOC dataset. However, the results cannot be directly compared without  
595 assessing the error that slacking of constraints (26) and (27) imposes on the CHOP solution.

596 By applying the optimal operation pattern predicted by the CHOP solution on the chronological EOC  
597 dataset, it is possible to evaluate the contents of the thermal energy storage over the 5-year period  
598 investigated. A plot of the thermal energy storage contents over the 5-year period for the optimal solutions  
599 to problem (28) obtained using the full EOC dataset and the revised CHOP dataset is presented in Figure 15.

600 It is seen that the CHOP solution significantly violates the physical constraints of the thermal energy storage  
601 in the model over the 5-year period. The explanation is quite simple: When slacking constraints (26) and  
602 (27), the only constraint on the heat production is that heat production and consumption must be balanced  
603 over the entire period. As the power prices on average were higher in the first two years of the period  
604 (consult Table 12 in the Appendix), power production is maximized at the cost of heat production in 2010  
605 and 2011, while excess heat is produced the following years when power prices are lower. It can also be

606 deducted from the graph that additional heat is produced in the summer periods when demand is low, and  
607 then stored for use in the winter when heat demand is high. Though highly intuitive, this solution is  
608 infeasible in reality due to thermal energy storage constraints. The results illustrates that the CHOP method  
609 may not be suitable for data reduction in models where short-term thermal energy storage is considered.

#### 610 **4. Discussion and perspective**

611 As the optimization of FMG concepts is complex and involves such challenges as synthesising and  
612 dimensioning of processes, process integration, and operation optimization, it is desirable to reduce  
613 external operating condition (EOC) datasets to be used in multi-period optimization models in order to  
614 make the models solvable. The CHOP method presented in this paper is a simple method for reducing EOC  
615 datasets by clustering data points in groups. The main advantages of the CHOP method include the  
616 significant reduction in the size of input data to multi-period optimization problems and the consequent  
617 reduction in computation costs, the simple and straight-forward use, and the fact that short-term relations  
618 and variations between various operating conditions are sustained in CHOP-reduced dataset.

619 For the simple case study presented in this paper, which treated the operation optimization of a fictive  
620 Danish CHP plant, it was found that the solution obtained using the revised CHOP-reduced EOC dataset had  
621 a much higher accuracy in terms of economic result and estimations of power production and fuel  
622 consumption than the solutions obtained using chronology-averaged EOC datasets. Furthermore, it was  
623 found that the revised CHOP dataset reduced the relative amount of computations by approximately a  
624 factor 827, which is comparable to the reductions of approximately a factor 730 when using monthly  
625 averaged dataset and approximately a factor 1096 when using the peak/off-peak averaged dataset. For the  
626 simple case, the advantage of the reduction in computation costs was not evident as the linear  
627 optimization problem could be solved within a minute using the full dataset. However, if more advanced  
628 optimization models needed be evaluated, e.g. non-linear operation optimization models, and if these  
629 further needed be solved for a large number of different designs for each operating point as in the design  
630 optimization of complex FMGs, reductions in computation costs is needed. Hence, the combination of high

631 accuracy and significant reduction in computation time support the proposition that the CHOP method is  
632 relevant for reducing EOC datasets to be used in optimization models of FMGs, and that the method is to  
633 be preferred over any of the three averaging methods mentioned in this paper.

634 The advantage of sustaining information on short-term parameter relations will assumedly be even more  
635 significant in more complex optimization models that consider multiple processes. For instance, if a process  
636 was considered for integration in the case study CHP plant which would only be economic advantageous to  
637 run when power prices are below 25.00 Euro/MWh, it would never be operated if annual or monthly  
638 averaged datasets were applied in the optimization model, while it would be run for 2192 hours over the  
639 five year period if the peak/off-peak averaged dataset was used, and for 4550 hours, or more than 10% of  
640 the time, if the CHOP-reduced dataset or the reference dataset were applied. Sustained data diversity in  
641 CHOP-reduced datasets thus allows for more accurate solutions. The fact that a large part of the initial  
642 dataset parameter diversity is sustained in the CHOP-reduced dataset is also evident from Figure 9, which  
643 illustrates how the parameter diversity in defined CHOP groups is significantly larger than for any of the  
644 three averaged datasets. Furthermore, for equipment with performance that is a non-linear function of an  
645 EOC parameter, e.g. the power production of a wind turbine as a function of the wind speed, the use of  
646 CHOP-reduced datasets rather than chronological-averaged datasets will assumedly yield more accurate  
647 results.

648 Another advantage of the CHOP method is the fact that larger datasets do not necessarily yield larger  
649 reduced datasets. In the case study, hourly heat demand and power price data were considered for a 5-  
650 year period. The initial 43,824 data points were reduced to 60 data points using the monthly averaging  
651 method, 40 data points using the seasonal peak/off-peak averaging method, and 53 using the CHOP  
652 method. If the period considered was extended to a 30-year period, the number of data points would be  
653 multiplied by six for each of the chronological-averaged methods, while it is likely that the number of  
654 CHOP-groups would not need to be changed. Instead, the weight given to each of the CHOP groups defined  
655 would increase as the additional data points are sorted into the groups. However, it is likely that the

656 increase in weight will not be the same for all CHOP groups due to the development of the energy system.

657 If the time-value of money needs to be considered, the time weight given to each sorted data point can be

658 replaced by a present value weight factor, as discussed in section 2.1.3., allowing for net present value

659 calculations in design optimization models.

660 Error analysis is central in the CHOP method as it provides the feedback required to optimize the data

661 aggregation strategy. In the present work, a number of approaches for conducting the error analysis were

662 suggested. However, it must be emphasized that other methods may be applied as long as they do not

663 counteract the initial ambition of reducing overall computation time. One example of a method that may

664 be useful for error analysis in the CHOP method is the global sensitivity analysis Morris Screening [50],

665 which could be applied *a posteriori* for assessing the quality of the defined characteristic interval breaks by

666 estimating the aggregated impact of varying EOC parameters within the defined intervals, or to evaluate if

667 a non-clustering EOC parameter ought to be included in the clustering analysis.

668 Two significant draw-backs exist for the CHOP method. Firstly, the number of CHOP groups defined is

669 combinatorial as a function of the relevant EOC parameters defined for a given problem. In the case study,

670 three EOC parameters were considered, of which one was excluded from the clustering analysis, and seven

671 and eight characteristic intervals were defined for the other two, resulting in 56 potential CHOP groups

672 according to equation (2). However, if two additional EOC parameters were considered for clustering with

673 four characteristic intervals each, the number of potential CHOP groups would increase to 896. Even

674 though the final number of CHOP groups may be lower according to equation (7), the combinatorial issue

675 represents a significant challenge when applying the CHOP method on datasets with multiple EOC

676 parameters. This also explains why it is relevant to seek to exclude less volatile parameters from the CHOP

677 data aggregation in the entity selection. One way of circumventing the combinatorial issue is to set up

678 relations for deriving various parameters from a few EOC parameters. For example, it may be possible to

679 derive formulas for heating and cooling demands as a function of the outdoor temperature [51] or the cost

680 of various fuels as a function of the expected oil price [2]. If such relations are introduced, the uncertainty

681 of the applied relations should be included in the sensitivity and error analyses conducted for results  
682 obtained.

683 Secondly, the CHOP method does not permit consideration of dynamics and time chronology directly,  
684 which is also the case for yearly- and monthly-averaged datasets. This implies that ramp constraints on  
685 operation cannot be considered, potentially resulting in infeasible operation patterns as discussed by Rong  
686 and Lahdelma [52], and that thermal energy storages cannot be directly included, as discussed in section  
687 3.5. Also, scheduling of maintenance shut-downs cannot be considered when using CHOP-reduced datasets,  
688 and neither can investment planning if the entire reference dataset is reduced to a single CHOP-reduced  
689 dataset. The latter can be solved by setting a time-span for investment planning, e.g. 5 years, and then  
690 derive a CHOP-reduced dataset for every 5-year period. However, this would increase the size of the  
691 dataset significantly, counteracting one of the initial advantages of the CHOP-method.

692 To overcome the challenges of including thermal energy storage and ramp constraints, it is suggested that  
693 CHOP-reduced datasets, rather than yearly or monthly reduced datasets, are applied in a first-step design  
694 optimization run, and that a detailed operation optimization is carried out in a sequential step for the most  
695 promising designs, similar to the method presented by Rubio-Maya et al. [22] and Uche et al. [23].

## 696 **5. Conclusion**

697 This study presents a novel and simple method, the Characteristic Operating Pattern (CHOP) method, for  
698 reducing external operating condition (EOC) datasets in optimization models. The method has been tailored  
699 for optimization models of flexible multi-generation plants (FMGs), but may be suitable for any  
700 optimization model that involves a flexible facility operating on multiple markets.

701 In a case study, an operation optimization model of a Danish extraction-based combined heat and power  
702 plant is solved using the full EOC dataset, a CHOP-reduced EOC dataset, a yearly-averaged EOC dataset, a  
703 monthly-averaged EOC dataset, and a seasonal peak/off-peak EOC dataset. The results indicate that the  
704 CHOP-reduced dataset yields by far the most accurate solution among all the reduced EOC datasets, while  
705 achieving a reduction in the problem size similar to those achieved of using monthly-averaged and seasonal

706 peak/off-peak-averaged datasets. It is found that CHOP-reduced datasets are not suited for models that  
707 consider short-term thermal energy storage as time chronology is not considered.  
708 The outcomes of the paper suggest that the CHOP method is better suited for reducing EOC datasets in  
709 optimization models of FMGs than any of the three chronology-averaged methods used for comparison in  
710 this paper. If short-term thermal energy storage or ramp constraints are considered, it is suggested that the  
711 CHOP method is applied in a first-step design optimization method, and that detailed operation  
712 optimization, including dynamic constraints, is carried out in a sequential step for the most promising  
713 designs. The latter will be a topic for future research by our group.

## 714 **Acknowledgements**

715 The authors would like to acknowledge DONG Energy for their financial support of the research.

## 716 **References**

717

- [1] H. Lund, *Renewable energy systems: the choice and modelling of 100% renewable solutions*, Burlington, USA: Elsevier, 2010.
- [2] Y. Chen, T. A. Adams II and P. I. Barton, "Optimal Design and Operation of Flexible Energy Polygeneration Systems," *Industrial & Engineering Chemistry Research*, no. 50, pp. 4553-4566, 2011.
- [3] A. Coronas, S. S. Murthy and J. C. Bruno, "Editorial for the special issue of applied thermal engineering on polygeneration," *Applied Thermal Energy*, no. 50, pp. 1397-1398, 2013.
- [4] M. Gassner and F. Maréchal, "Increasing Efficiency of Fuel Ethanol Production from Lignocellulosic Biomass by Process Integration," *Energy Fuels*, no. 27, pp. 2107-2115, 2013.
- [5] O. Edenhofer, R. Pichs-Madruga and Y. Sokona, "Renewable Energy Sources and Climate Change Mitigation," Intergovernmental Panel on Climate Change and Cambridge University Press, New York, USA, 2012.
- [6] L. Daianova, E. Dotzauer, E. Thorin and J. Yan, "Evaluation of a regional bioenergy system with local production of biofuel for transportation, integrated with a CHP plant," *Applied Energy*, no. 92, pp. 739-749, 2011.
- [7] D. D. Ilic, E. Dotzauer and L. Trygg, "District heating and ethanol production through polygeneration in

Stockholm," *Applied Energy*, no. 91, pp. 214-221, 2011.

- [8] T. Kohl, M. Teles, K. Melin, T. Laukkanen, M. Järvinen, S. W. Park and R. Guidici, "Exergoeconomic assessment of CHP-integrated biomass upgrading," *Applied Energy*, no. 156, pp. 290-305, 2015.
- [9] B. Mathiesen, H. Lund, D. Connolly, H. Wenzel, P. Østergaard, B. Möller, S. Nielsen, I. Ridjan, P. Karnøe, K. Sperling and F. Hvelplund, "Smart Energy Systems for coherent 100% renewable energy and transport solutions," *Applied Energy*, no. 145, pp. 139-154, 2015.
- [10] B. Mathiesen, H. Lund, D. Connolly, H. Wenzel, P. Østergaard, B. Möller, S. Nielsen, I. Ridjan, P. Karnøe, K. Spelling and F. Hvelplund, "Smart Energy Systems for coherent 100% renewable energy and transport solutions," *Applied Energy*, no. 145, pp. 139-154, 2015.
- [11] D. Connolly, H. Lund, B. Mathiesen and M. Leahy, "A review of computer tools for analysing the integration of renewable energy in various energy systems," *Applied Energy*, no. 87, pp. 1059-1082, 2010.
- [12] M. Hindsberger and H. F. Ravn, "Multiresolution modeling of hydro-thermal systems," in *PICA: 22ND IEEE POWER ENGINEERING SOCIETY INTERNATIONAL CONFERENCE ON POWER INDUSTRY COMPUTER APPLICATIONS*, Sydney, Australia, 2001.
- [13] R. R. Iyer and I. E. Grossmann, "Synthesis and operational planning of utility systems for multiperiod operation," *Computers & Chemical Engineering*, no. 22, pp. 979-993, 1998.
- [14] P. Ahmadi, M. A. Rosen and I. Dincer, "Multi-objective exergy-based optimization of a polygeneration energy system using an evolutionary algorithm," *Energy*, no. 46, pp. 21-31, 2012.
- [15] M. Gassner and F. Maréchal, "Thermo-economic optimisation of the polygeneration of synthetic natural gas (SNG), power and heat from lignocellulosic biomass by gasification and methanation," *Energy & Environmental Science*, no. 5, pp. 5768-5789, 2012.
- [16] Y. Chen, T. A. Adams II and P. I. Barton, "Optimal Design and Operation of Static Energy Polygeneration Systems," *Industrial & Engineering Chemistry Research*, no. 50, pp. 5099-5113, 2010.
- [17] P. Liu, D. I. Gerogiorgis and E. N. Pistikopoulos, "Modeling and optimization of polygeneration energy systems," *Catalysis Today*, no. 127, pp. 347-359, 2007.
- [18] P. Liu, E. N. Pistikopoulos and Z. Li, "A Multi-Objective Optimization Approach to Polygeneration Energy Systems Design," *Process Systems Engineering*, no. 56, pp. 1218-1234, 2010.
- [19] P. Liu, E. N. Pistikopoulos and Z. Li, "Environmentally Benign Process Design of Polygeneration Energy Systems," in *Design for Energy and the Environment*, Taylor and Francis Group, LLC, 2010, pp. 585-592.
- [20] S. Fazlollahi, P. Mandel, G. Becker and F. Maréchal, "Methods for multi-objective investment and



operating optimization of complex energy systems," *Energy*, no. 45, pp. 12-22, 2012.

- [21] S. Fazlollahi and F. Maréchal, "Multi-objective, multi-period optimization of biomass conversion technologies using evolutionary algorithms and mixed integer linear programming (MILP)," *Applied Thermal Engineering*, no. 50, pp. 1504-1513, 2013.
- [22] C. Rubio-Maya, J. Uche-Marcuello, A. Martín-García and A. A. Bayod-Rújula, "Design optimization of a polygeneration plant fuelled by natural gas and renewable energy sources," *Applied Energy*, no. 88, pp. 449-457, 2011.
- [23] C. Rubio-Maya, J. Uche and A. Martínez, "Sequential optimization of a polygeneration plant," *Energy Conversion and Management*, no. 52, pp. 2861-2869, 2011.
- [24] A. Christidis, C. Koch, L. Pottel and G. Tsatsaronis, "The contribution of heat storage to the profitable operation of combined heat and power plants in liberalized electricity markets," *Energy*, no. 41, pp. 75-82, 2011.
- [25] C. Lythcke-Jørgensen, F. Haglind and L. R. Clausen, "Exergy analysis of a combined heat and power plant with integrated lignocellulosic ethanol production," *Energy Conversion and Management*, no. 85, pp. 817-827, 2014.
- [26] C. Lythcke-Jørgensen and F. Haglind, "Design optimization of a polygeneration plant producing power, heat, and lignocellulosic ethanol," *Energy Conversion and Management*, no. 91, pp. 353-366, 2015.
- [27] C. Lythcke-Jørgensen, M. Münster, A. V. Ensinas and F. Haglind, "Design optimization of flexible biomass-processing polygeneration plants using characteristic operation periods," in *World Renewable Energy Congress XIII*, Kingston-upon-Thames, London, 2014.
- [28] Y. Chen, T. A. Adams II and P. I. Barton, "Decomposition Strategy for the Global Optimization of Flexible Energy Polygeneration Systems," *American Institute of Chemical Engineers*, no. 58, pp. 3080-3095, 2012.
- [29] G. Mavrotas, D. Diakoulaki, K. Florios and P. Georgiou, "A mathematical programming framework for energy planning in services' sector buildings under uncertainty in load demand: The case of a hospital in Athens," *Energy Policy*, no. 36, pp. 2415-2429, 2008.
- [30] J. Ortiga, J. Bruno and A. Coronas, "Selection of typical days for the characterisation of energy demand in cogeneration and trigeneration optimisation models for buildings," *Energy Conversion and Management*, no. 52, pp. 1934-1942, 2011.
- [31] F. Domínguez-Moñoz, J. M. Cejudo-López, A. Carrilo-Andrés and M. Gallardo-Salazar, "Selection of typical demand days for CHP optimization," *Energy and Buildings*, no. 43, pp. 3036-3043, 2011.
- [32] S. Fazlollahi, S. L. Bungener, P. Mandel, G. Becker and F. Maréchal, "Multi-objectives, multi-period optimization of district energy systems: I. Selection of typical operating periods," *Computers and*

*Chemical Engineering*, no. 65, pp. 54-66, 2014.

- [33] K. Hedegaard and M. Münster, "Influence of individual heat pumps on wind power integration – Energy system investments and operation," *Energy Conversion and Management*, no. 75, pp. 673-684, 2013.
- [34] S. Bungener, R. Hackl, G. V. Eetvelde, S. Harvey and F. Marechal, "Multi-period analysis of heat integration measures in industrial clusters," *Energy*, (in press).
- [35] A. Nemet, J. J. Klemes, P. S. Varbanov and Z. Kravanja, "Methodology for maximising the use of renewables with variable availability," *Energy*, no. 44, pp. 29-37, 2012.
- [36] DTU Management Engineering; Danish Energy Agency, 1 December 2013. [Online]. Available: [http://www.ens.dk/sites/ens.dk/files/info/facts-figures/scenarios-analyses-models/models/IntERACT/wp03\\_-\\_interact\\_times-dk\\_phase\\_1.pdf](http://www.ens.dk/sites/ens.dk/files/info/facts-figures/scenarios-analyses-models/models/IntERACT/wp03_-_interact_times-dk_phase_1.pdf). [Accessed 7 July 2015].
- [37] Nord Pool Spot, "Nord Pool Spot," [Online]. Available: <http://www.nordpoolspot.com/#/nordic/table>. [Accessed 4 November 2014].
- [38] M. W. Jack, "Scaling laws and technology development strategies for biorefineries and bioenergy plants.," *Bioresource Technology*, no. 100, pp. 6324-6330, 2009.
- [39] International Energy Agency, "Key World Energy STATISTICS 2014," International Energy Agency, Paris, 2014.
- [40] C. Lythcke-Jørgensen, "Modelling and Optimization of a Steam Co-generation Plant with Integrated Bio-ethanol Production," Technical University of Denmark, Kgs. Lyngby, 2012.
- [41] Energinet.dk, "Market data," Nord Pool Spot, [Online]. Available: [energinet.dk](http://energinet.dk). [Accessed 28 January 2015].
- [42] <http://www.streammodel.org/>, "The STREAM modelling tool," Ea Energy Analyses. [Online]. [Accessed 3 April 2014].
- [43] B. Elmegaard and N. Houbak, "Simulation of the Avedøreværket Unit 1 cogeneration plant with DNA," in *16th International Conference on Efficiency, Cost, Optimization, Simulation and Environmental Impact of Energy Systems*, DK-2800 Kgs. Lyngby, 2003.
- [44] H. Spliethoff, *Power Generation from Solid Fuels*, München, Germany: Springer-Verlag Berlin Heidelberg, 2010.
- [45] B. Elmegaard and N. Houbak, "DNA - A General Energy System Simulation Tool," in *SIMS*, 2005.
- [46] J. Forrest and R. Lougee-Heimer, "CBC User Guide," 2015. [Online]. Available: <http://www.coin->

or.org/Cbc/.

- [47] OpenSolver, OpenSolver, 2015. [Online]. Available: opensolver.org.
- [48] B. Rolfsman, "Combined heat-and-power plants and district heating in a deregulated electricity market," *Applied Energy*, no. 78, pp. 37-52, 2004.
- [49] S. Martínéz-Lera, J. Ballester and J. Martínéz-Lera, "Analysis and sizing of thermal energy storage in combined heating, cooling and power plants for buildings," *Applied Energy*, no. 106, pp. 127-142, 2013.
- [50] M. D. Morris, "Factorial Sampling Plans for Preliminary Computational Experiments," *Technometrics*, vol. 33, no. 2, pp. 161-174, 1991.
- [51] S. Frederiksen and S. Werner, "Heat and cold loads," in *District Heating and Cooling*, Lund, Sweden, Studentlitteratur AB, 2013, pp. 67-112.
- [52] A. Rong and R. Lahdelma, "An effective heuristic for combined heat-and-power production planning with power ramp constraints," *Applied Energy*, no. 84, pp. 307-325, 2007.

718

719

## 720 **Appendix**

721 This appendix presents the reduced external operating condition (EOC) datasets  $D_{AA}$  (Table 12),  $D_{MA}$

722 (Tables 13-15), and  $D_{SP}$  (Tables 16-18) as explained in Section 3.2.

Figure 1

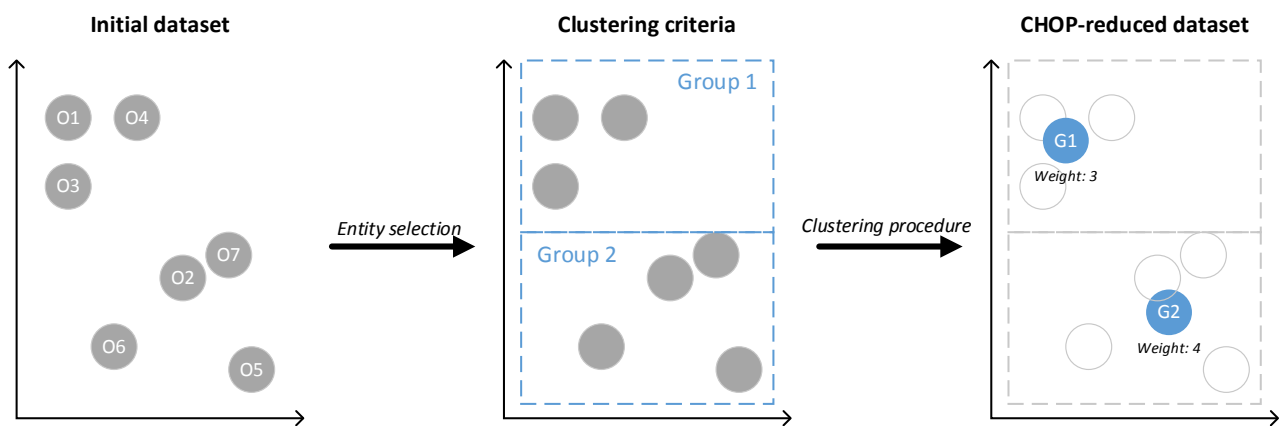


## Figure 1 Caption

Figure 1 – Principal sketch of the data aggregation principle applied in the CHOP method. Operating points  $O_j$  are clustered and merged into CHOP groups  $G_j$  with aggregated weight factors.

Figure 2

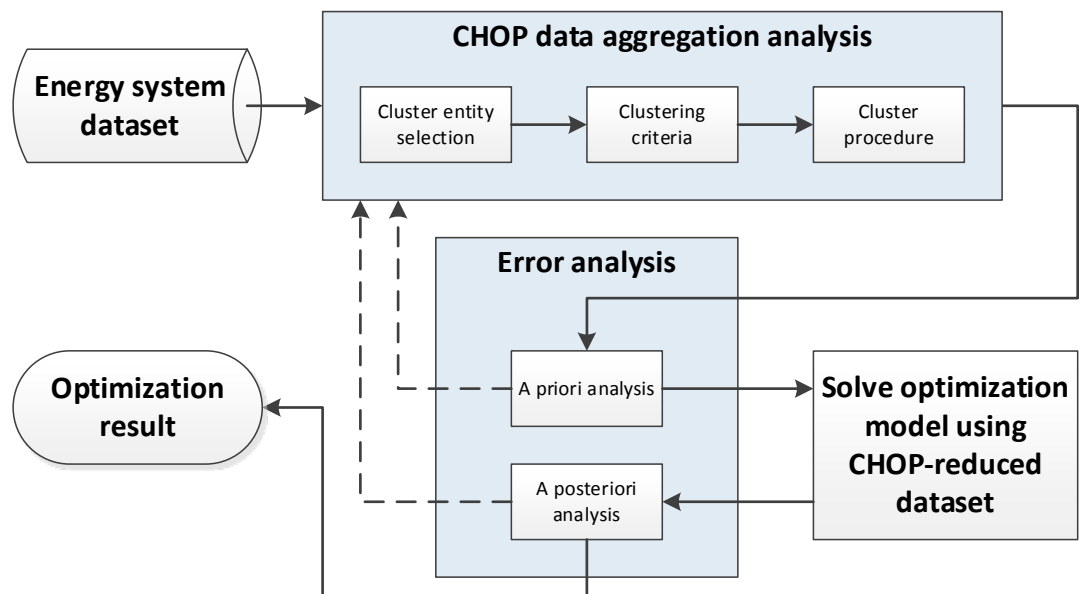


Figure 2 – The CHOP method procedure.

Figure 3

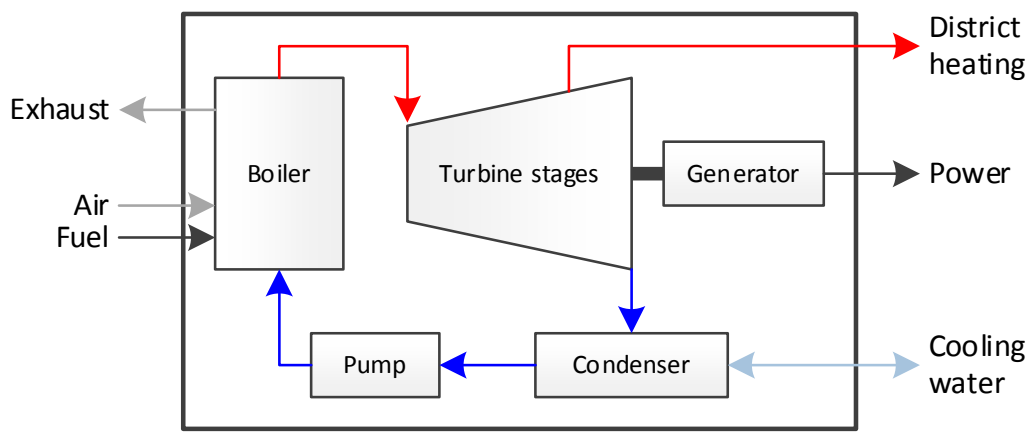
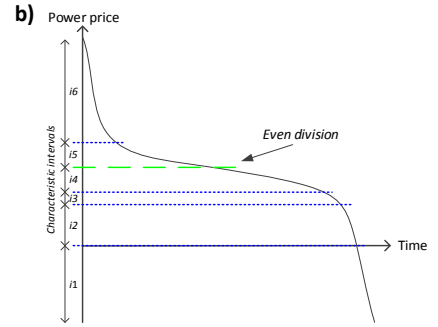
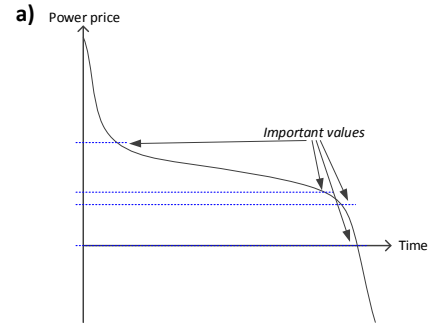
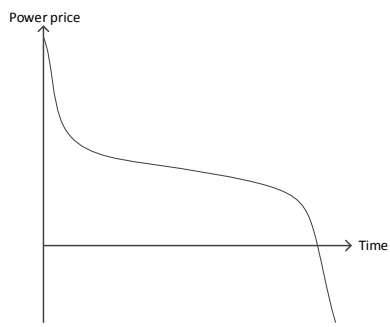




Figure 3 – Principal sketch of a Danish extraction-based CHP plant.

Figure 4



## Figure 4 Caption

Figure 4 – Illustrative example of the suggested two-step approach for defining characteristic intervals based on the cumulative curve (left). Interval break points are set for a) Important values, and b) Even division. The characteristic intervals are indicated on the second axis in b).

Figure 5

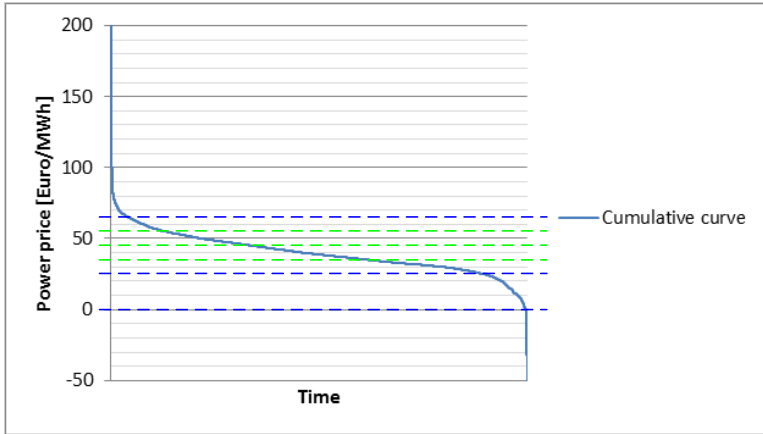


## Figure 5 Caption

Figure 5 – Cumulative curve for the power price in West Denmark over the period 2010-01-01 – 2014-12-31, with interval break lines.

Figure 6

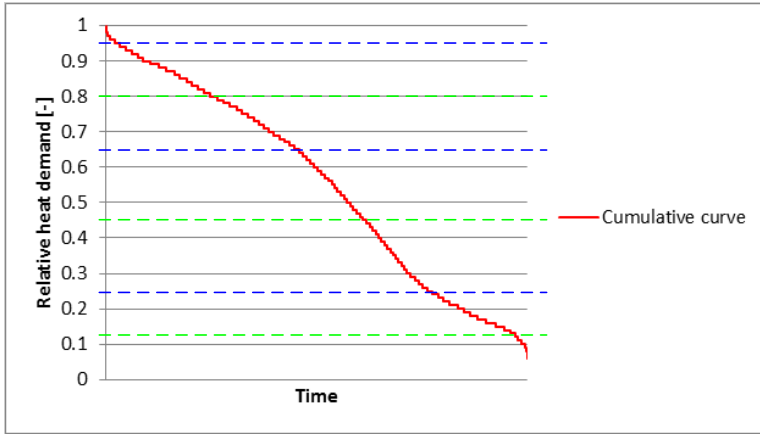


## Figure 6 Caption

Figure 6 – Cumulative curve for the relative heat demand in Denmark over the period 2010-01-01 – 2014-12-31, with interval break lines.

Figure 7

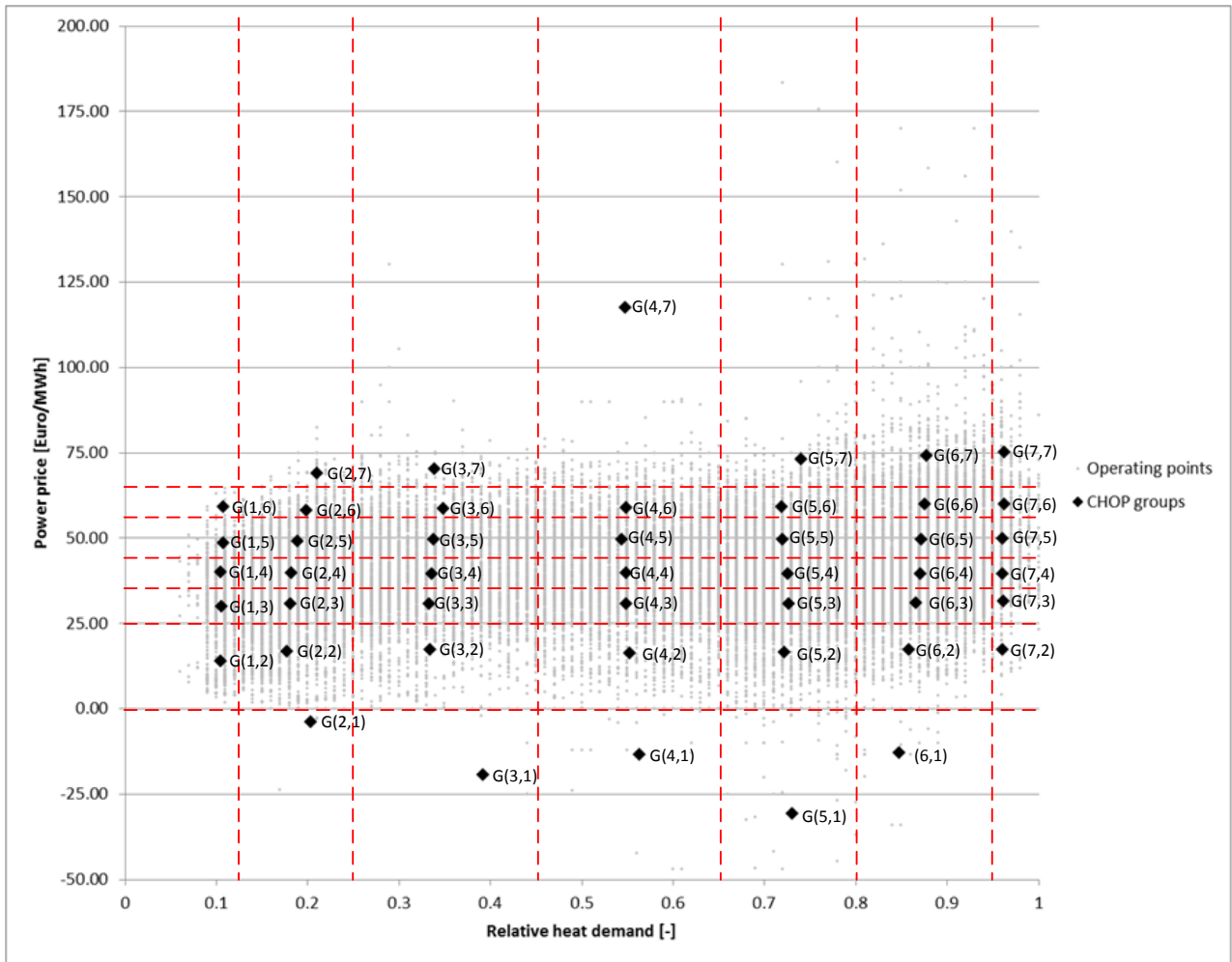




## Figure 7 Caption

Figure 7 – Scatter diagram showing the reference operating points, characteristic interval breaks, and final CHOP groups. Notice that a small number of the reference operating points lies outside the power price boundaries of the diagram.

Figure 8

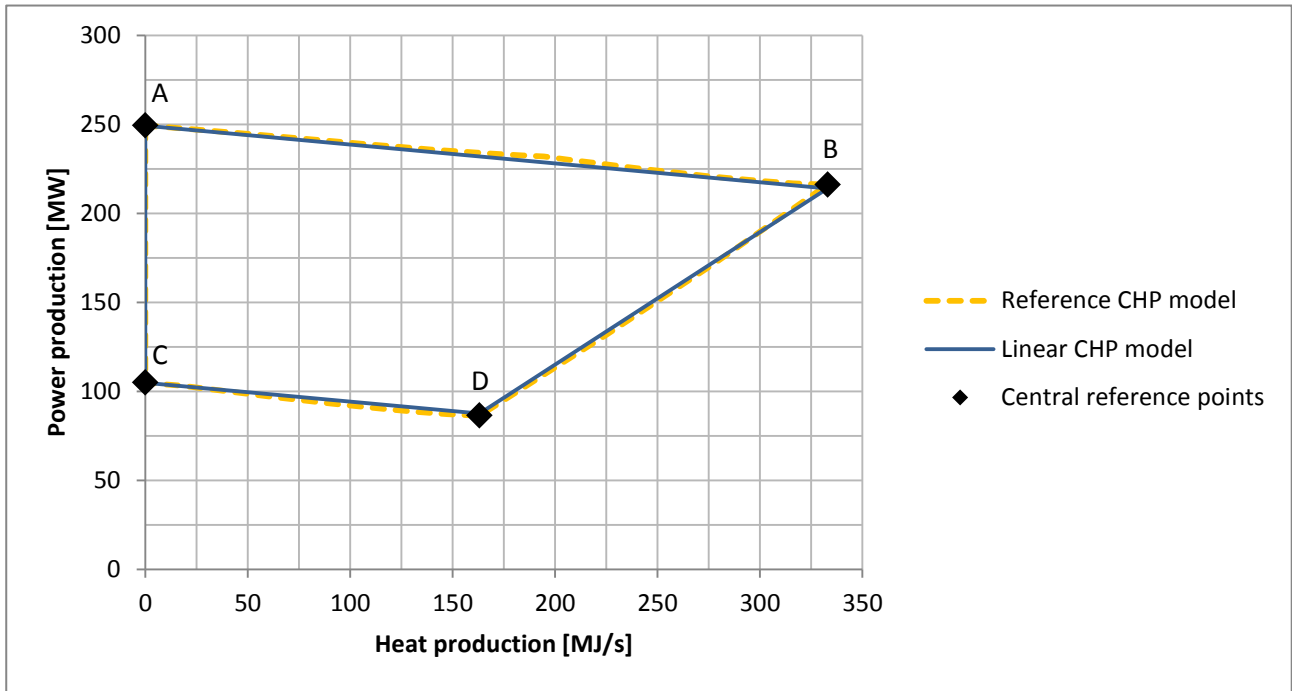
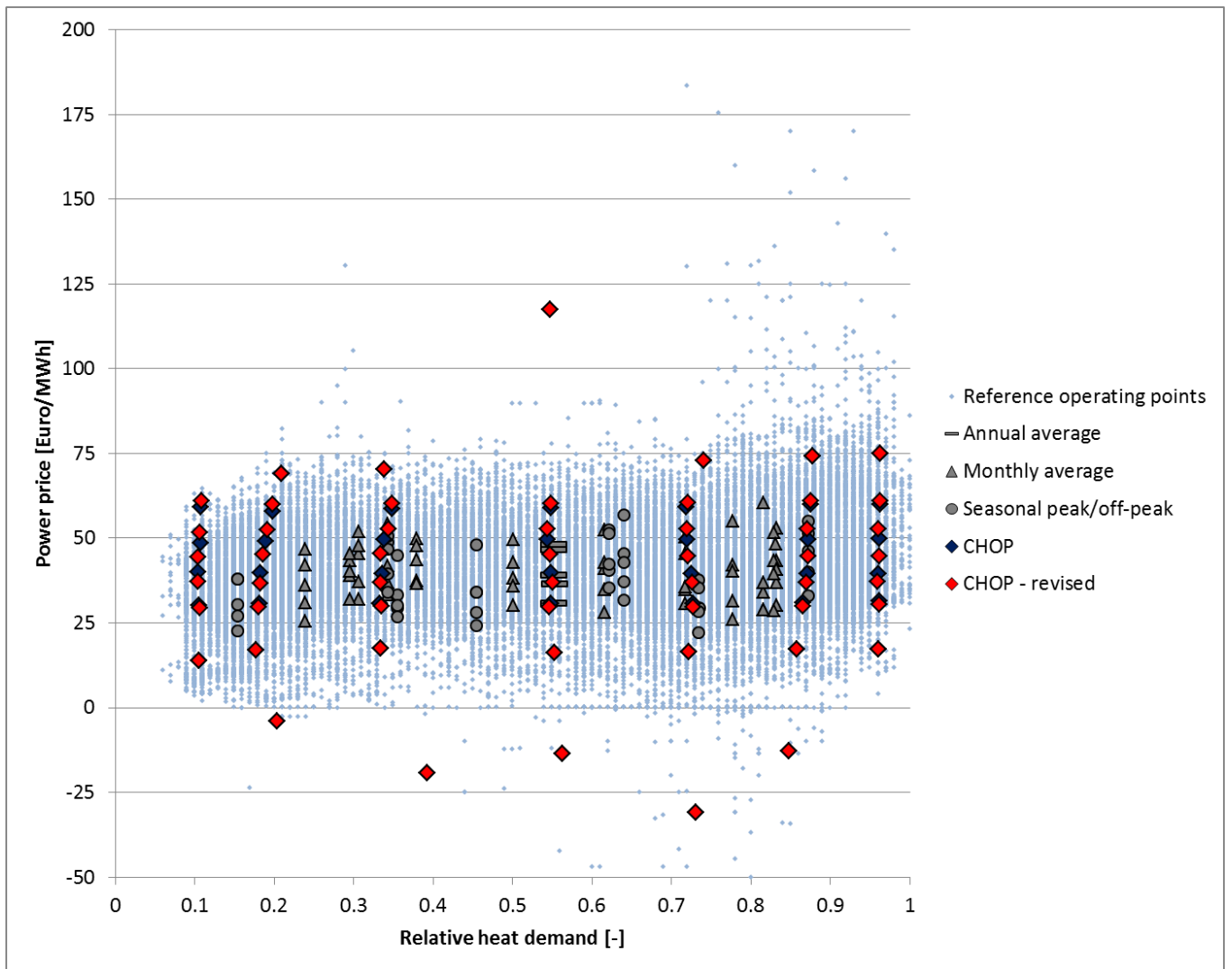


Figure 8 – Heat and power production range of the reference CHP plant model [43] and the developed linearized model. The outlined areas represent the feasible production points of the models. Four central operating points {A, B, C, D} are highlighted. Data for these operating points is presented in Table 6.

Figure 9



## Figure 9 Caption

Figure 9 – Scatter diagram showing reference, annually averaged, monthly averaged, seasonal peak/off-peak, CHOP, and revised-CHOP operating points over the period 2010-01-01 – 2014-12-31. Notice that some of the CHOP and revised-CHOP operating points are overlapping.

Figure 10

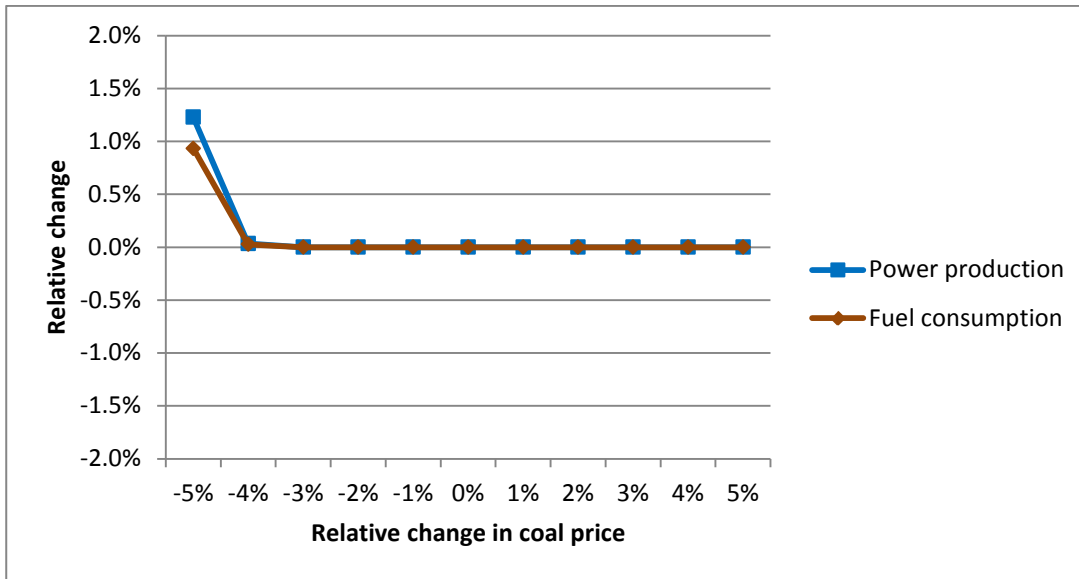


## Figure 10 Caption

Figure 10 – Relative changes in optimized power production and fuel consumption as a function of relative changes in the coal price. Notice that heat production is unaffected by the coal price as it is constrained in the optimization model.

Figure 11

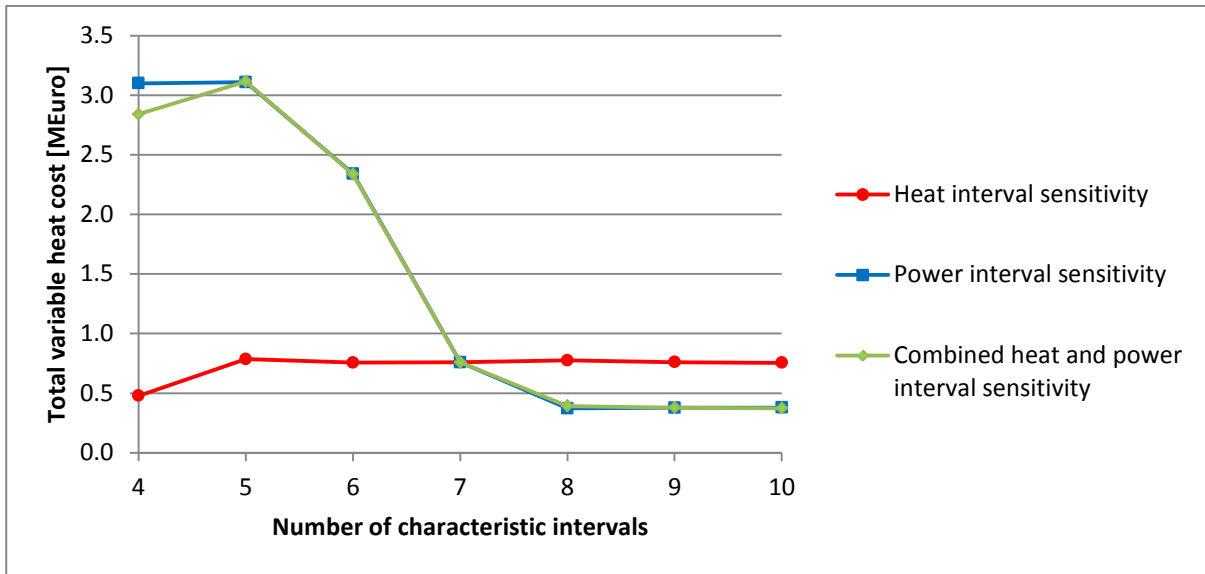




Figure 11 – Total variable heat cost sensitivity analysis.

Figure 12

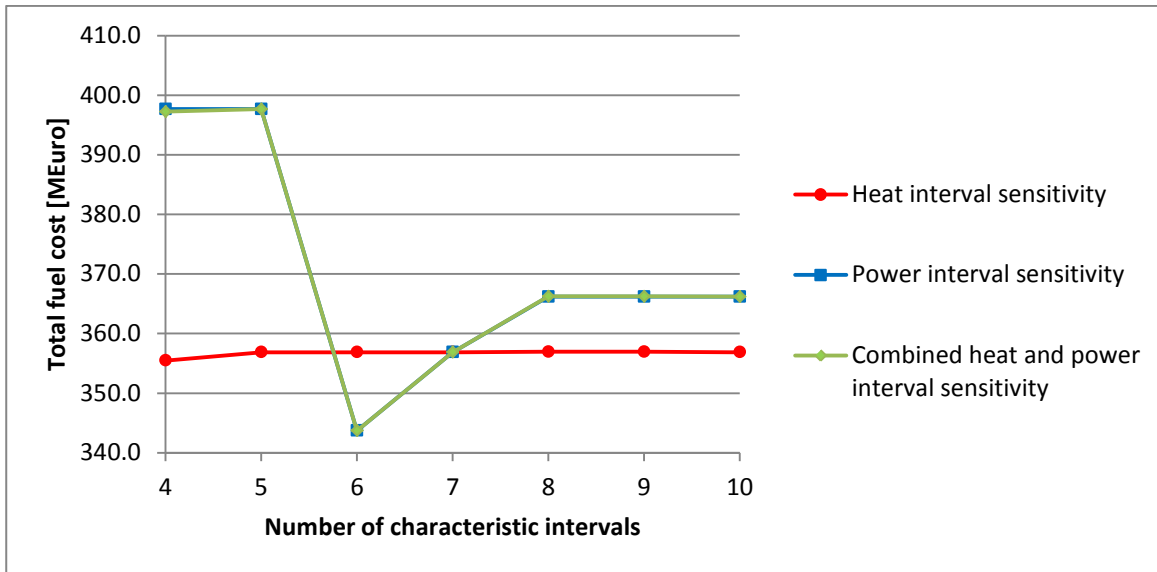


Figure 12 – Total fuel cost sensitivity analysis.

Figure 13

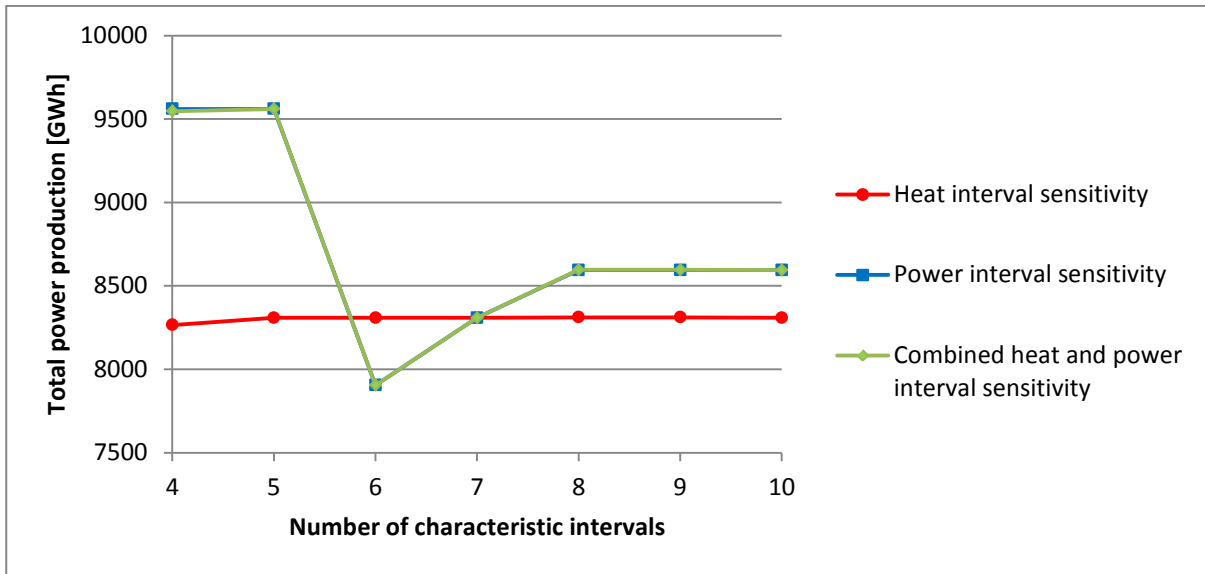


Figure 13 – Total power production sensitivity analysis.

Figure 14

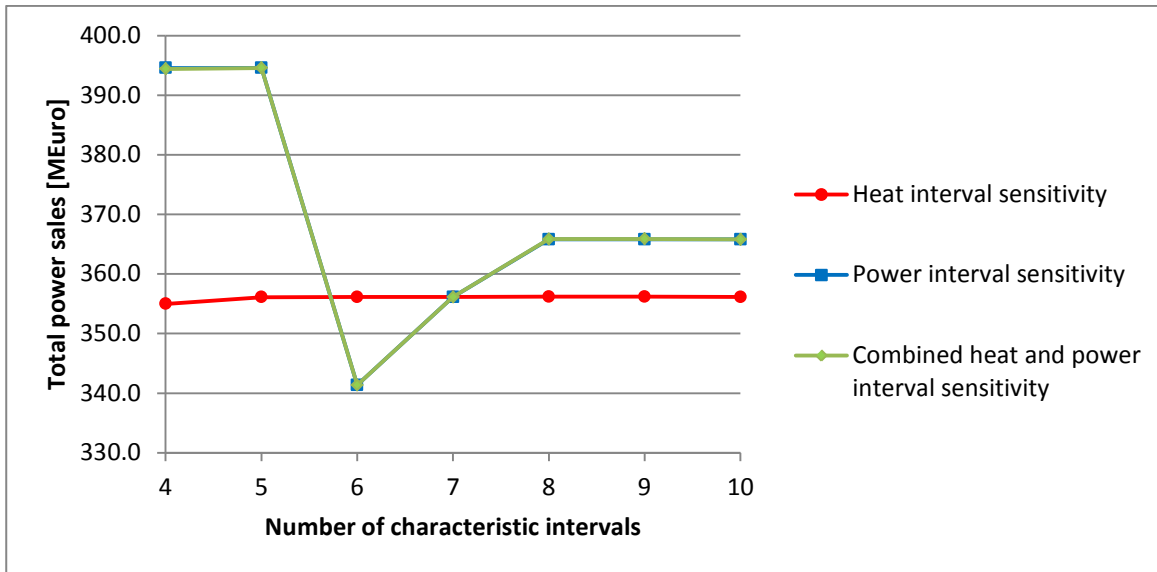
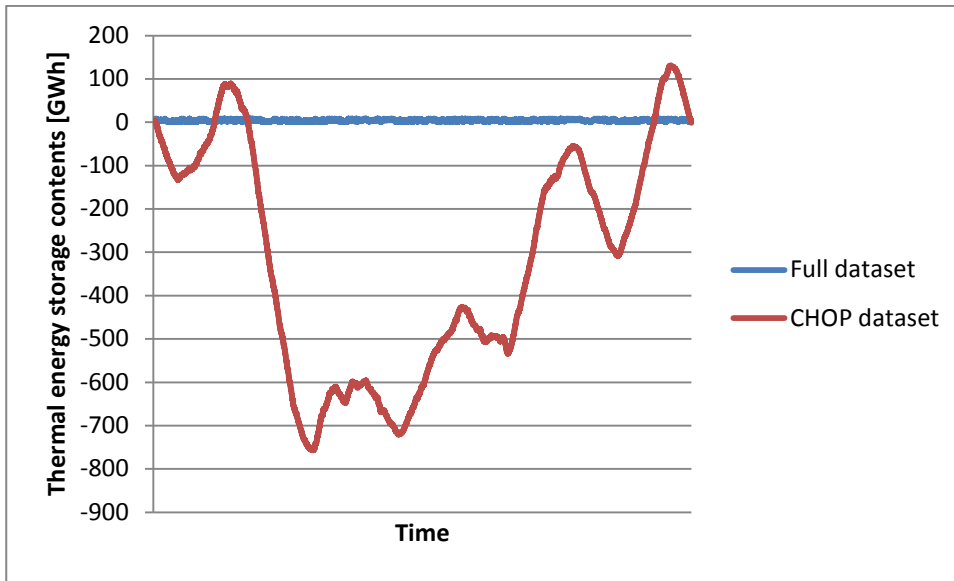


Figure 14 – Total power sales sensitivity analysis.

Figure 15





## Figure 15 Caption

Figure 15 – Thermal energy storage contents over the 5-year period for the optimal solutions to problem (27) obtained using the full EOC dataset and the revised CHOP dataset.

Table 1 – Characteristic power price intervals.

Power price interval number $i$	Smallest value [Euro/MWh]	Largest value [Euro/MWh]
1	$-\infty^a$	-0.01
2	0.00	24.99
3	25.00	34.99
4	35.00	44.99
5	45.00	54.99
6	55.00	64.99
7	65.00	$\infty^a$

<sup>a</sup> Notice that the intervals are defined as open towards the infinite to cover all feasible power prices

*Table 2 – Characteristic heat demand intervals.*

Heat demand interval number $i$	Smallest value [-]	Largest value [-]
1	0.000	0.124
2	0.125	0.249
3	0.250	0.449
4	0.450	0.649
5	0.650	0.799
6	0.800	0.949
7	0.950	1.000

Table 3 – Characteristics of the defined CHOP groups.

CHOP group characteristics							
Duration [h]	Power interval						
Heat interval	1	2	3	4	5	6	7
1	0	321	427	390	136	16	0
2	11	1178	2812	2327	1838	379	55
3	9	615	1808	1826	1739	640	178
4	22	717	1847	1828	1672	741	198
5	72	947	2380	2436	1649	803	273
6	30	582	2608	2932	1871	1158	903
7	0	46	262	442	272	217	211
Relative heat demand [-]							
1	-	0.105	0.106	0.104	0.107	0.108	-
2	0.204	0.178	0.181	0.183	0.189	0.199	0.210
3	0.392	0.334	0.333	0.336	0.338	0.348	0.339
4	0.563	0.553	0.548	0.549	0.544	0.549	0.547
5	0.731	0.721	0.727	0.726	0.720	0.719	0.740
6	0.848	0.858	0.866	0.871	0.872	0.875	0.878
7	-	0.961	0.961	0.960	0.961	0.963	0.963
Power price [Euro/MWh]							
1	-	13.91	30.06	40.14	48.52	59.09	-
2	-3.92	16.86	30.65	39.70	49.04	58.00	69.02
3	-19.24	17.43	30.77	39.43	49.58	58.53	70.32

<b>4</b>	-13.46	16.22	30.78	39.78	49.48	58.99	117.54
<b>5</b>	-30.81	16.58	30.73	39.54	49.58	59.13	72.97
<b>6</b>	-12.90	17.36	31.01	39.58	49.60	59.90	74.10
<b>7</b>	-	17.20	31.54	39.56	49.74	60.00	75.08

Table 4 – CHOP group relative heat demand standard deviation,  $\sigma_{\lambda_{heat}}$ .

CHOP group $\sigma_{\lambda_{heat}}$ [-]							
Heat interval \ power interval	1	2	3	4	5	6	7
1	-	0.011	0.012	0.012	0.012	0.011	-
2	0.026	0.032	0.032	0.033	0.031	0.029	0.020
3	0.065	0.058	0.059	0.060	0.061	0.058	0.059
4	0.055	0.058	0.058	0.058	0.059	0.060	0.061
5	0.040	0.041	0.044	0.044	0.043	0.045	0.044
6	0.038	0.042	0.042	0.042	0.042	0.042	0.042
7	-	0.011	0.013	0.012	0.013	0.014	0.013

Table 5 – CHOP group power price standard deviation,  $\sigma_{c_{power}}$ .

CHOP group $\sigma_{c_{power}}$ [Euro/MWh] Heat interval \ power interval	1	2	3	4	5	6	7
1	-	6.57	2.70	2.80	2.37	3.14	-
2	6.35	6.45	2.63	2.90	2.76	2.67	3.61
3	21.67	6.64	2.66	2.89	2.82	2.82	7.49
4	16.79	6.91	2.70	2.87	2.78	2.82	293.62
5	55.98	7.23	2.64	2.87	2.91	2.75	14.17
6	16.10	6.42	2.54	2.78	2.86	3.07	13.46
7	-	4.61	2.31	2.83	2.96	2.87	11.07

Table 6 – Data on four central reference points {A, B, C, D} in the reference model of AVV1 [43], and their corresponding points {A\*, B\*, C\*, D\*} in the linearized model of AVV1.

Point, $j$	Load, $\lambda$	Back-pressure ratio, $\alpha$	Power production, $P_j$ [MW]	Heat production, $Q_j$ [MJ/s]
A	1.0	0.0	249.3	0.0
A*	1.0	0.0	249.3	0.0
B	1.0	1.0	216.0	332.9
B*	1.0	1.0	213.9	332.9
C	0.4	0.0	104.9	0.0
C*	0.4	0.0	104.9	0.0
D	0.4	1.0	86.3	163.1
D*	0.4	1.0	87.5	163.1



Table 7 – Optimization results obtained using the five different EOC datasets.

	Full dataset	Annually averaged	Monthly averaged	Seasonal peak/off-peak	CHOP- reduced
RESULTS					
Total variable heat cost, $C_{heat}$ [MEuro]	0.38	8.53	8.02	5.96	0.76
Total power sales [MEuro]	368.06	369.51	376.62	370.41	356.12
Total fuel costs [MEuro]	368.44	377.81	384.64	376.38	356.88
PRODUCTION DATA					
Total heat production [GWh]	8,066	8,066	8,066	8,066	8,066
Total power production [GWh]	8,664	8,958	9,161	8,907	8,309
Total fuel consumption [GWh]	23,460	24,057	24,492	23,966	22,724
OPTIMIZATION PROBLEM					
Number of periods	43,824	5	60	40	46
Variables per period	2	2	2	2	2
Constraints per period	4	4	4	4	4



Table 9 – Characteristics of the revised CHOP groups.

CHOP group characteristics								
Duration [h]	Power interval							
Heat interval	1	2	3	4	5	6	7	8
1	0	321	356	306	242	55	10	0
2	11	1178	2198	2111	1872	980	195	55
3	9	615	1383	1673	1400	1150	407	178
4	22	717	1402	1600	1483	1085	518	198
5	72	947	1824	2163	1565	1139	577	273
6	30	582	1953	2641	1776	1301	898	903
7	0	46	189	365	267	195	177	211
<b>Relative heat demand [-]</b>								
1	-	0.105	0.106	0.105	0.105	0.107	0.109	-
2	0.204	0.178	0.180	0.182	0.186	0.191	0.199	0.210
3	0.392	0.334	0.335	0.334	0.334	0.344	0.348	0.339
4	0.563	0.553	0.546	0.550	0.547	0.544	0.549	0.547
5	0.731	0.721	0.727	0.726	0.721	0.720	0.721	0.740
6	0.848	0.858	0.866	0.870	0.872	0.871	0.876	0.878
7	-	0.961	0.961	0.960	0.962	0.961	0.963	0.963
<b>Power price [Euro/MWh]</b>								
1	-	13.91	29.32	37.20	44.49	51.62	61.11	-
2	-3.92	16.86	29.73	36.73	45.20	52.51	60.05	69.02
3	-19.24	17.43	29.80	36.80	45.40	52.64	60.23	70.32

<b>4</b>	-13.46	16.22	29.77	36.83	45.20	52.59	60.34	117.54
<b>5</b>	-30.81	16.58	29.75	36.82	44.74	52.63	60.39	72.97
<b>6</b>	-12.90	17.36	30.03	36.98	44.76	52.59	61.08	74.10
<b>7</b>	-	17.20	30.56	37.11	44.58	52.75	60.95	75.08

Table 10 – Optimization results obtained using the CHOP and the revised CHOP EOC datasets.

	Full dataset	CHOP	CHOP-revised
RESULTS			
Total variable heat cost, $C_{heat}$ [MEuro]	0.38	0.76	0.37
Total power sales [MEuro]	368.06	356.12	365.81
Total fuel costs [MEuro]	368.44	356.88	366.18
PRODUCTION DATA			
Total heat production [GWh]	8,066	8,066	8,066
Total power production [GWh]	8,664	8,309	8,594
Total fuel consumption [GWh]	23,460	22,724	23,317
OPTIMIZATION PROBLEM			
Number of periods	43,824	46	53
Variables per period	2	2	2
Constraints per period	4	4	4

Table 11 - Optimization results obtained from solving optimization problem (28) using the full EOC dataset and the revised CHOP dataset.

	Full dataset Problem (22)	Full dataset Problem (28)	CHOP-revised Problem (28)*
RESULTS			
Total variable heat cost, $C_{heat}$ [MEuro]	0.38	-6.08	-8.06
Total power sales [MEuro]	368.06	372.50	357.04
Total fuel costs [MEuro]	368.44	366.42	348.97
PRODUCTION DATA			
Total heat production [GWh]	8,066	8,066	8,066
Total power production [GWh]	8,664	8,602	8,066
Total fuel consumption [GWh]	23,460	23,332	22,221
OPTIMIZATION PROBLEM			
Number of periods	43,824	43,824	53
Variables per period	2	2	2
Constraints per period	4	6	4

\* Constraints (26) and (27) were slacked when solving optimization problem (28) using the CHOP-revised dataset.

Table 12 – Annually averaged EOC dataset,  $D_{AA}$ .

Year	Duration [h]	Power price, $c_{p,j}$ [Euro/MWh]	Relative heat demand, $q_j$ [-]
2010	8760	46.48	0.553
2011	8760	47.96	0.553
2012	8784	36.33	0.554
2013	8760	38.98	0.553
2014	8760	30.67	0.553

Table 13 – Monthly averaged EOC dataset,  $D_{MA}$ , period duration.

<b>Duration [h]</b>	<b>2010</b>	<b>2011</b>	<b>2012</b>	<b>2013</b>	<b>2014</b>
<b>January</b>	744	744	744	744	744
<b>February</b>	672	672	696	672	672
<b>March</b>	744	744	744	744	744
<b>April</b>	720	720	720	720	720
<b>May</b>	744	744	744	744	744
<b>June</b>	720	720	720	720	720
<b>July</b>	744	744	744	744	744
<b>August</b>	744	744	744	744	744
<b>September</b>	720	720	720	720	720
<b>October</b>	744	744	744	744	744
<b>November</b>	720	720	720	720	720
<b>December</b>	744	744	744	744	744



Table 14 – Monthly averaged EOC dataset,  $D_{MA}$ , period power price.

<b>Power price [Euro/MWh]</b>	<b>2010</b>	<b>2011</b>	<b>2012</b>	<b>2013</b>	<b>2014</b>
<b>January</b>	43.29	52.89	37.01	40.77	30.26
<b>February</b>	43.45	51.75	48.35	39.40	28.74
<b>March</b>	42.09	55.14	31.51	40.33	26.05
<b>April</b>	41.11	52.33	34.76	42.82	28.13
<b>May</b>	41.73	54.35	36.06	36.82	33.34
<b>June</b>	45.49	51.99	37.21	47.74	31.88
<b>July</b>	46.81	42.20	25.55	36.24	31.02
<b>August</b>	43.28	45.42	39.01	40.17	32.11
<b>September</b>	49.86	47.79	37.40	43.67	36.58
<b>October</b>	49.48	42.76	38.11	35.90	30.13
<b>November</b>	50.45	45.45	34.91	35.60	30.78
<b>December</b>	60.50	33.97	36.86	28.80	28.99

Table 15 – Monthly averaged EOC dataset,  $D_{MA}$ , period relative heat demand.

Relative heat demand[-]	2010	2011	2012	2013	2014
January	0.83	0.83	0.83	0.83	0.83
February	0.83	0.83	0.83	0.83	0.83
March	0.78	0.78	0.78	0.78	0.78
April	0.62	0.62	0.62	0.62	0.62
May	0.34	0.34	0.34	0.34	0.34
June	0.31	0.31	0.31	0.31	0.31
July	0.24	0.24	0.24	0.24	0.24
August	0.30	0.30	0.30	0.30	0.30
September	0.38	0.38	0.38	0.38	0.38
October	0.50	0.50	0.50	0.50	0.50
November	0.72	0.72	0.72	0.72	0.72
December	0.82	0.82	0.82	0.82	0.82

Table 16 – Seasonal averaged peak/off-peak averaged EOC dataset,  $D_{SP}$ , period duration.

<b>Duration [h]</b>	<b>2010</b>	<b>2011</b>	<b>2012</b>	<b>2013</b>	<b>2014</b>
<b>Winter, peak</b>	1440	1440	1456	1440	1440
<b>Winter, off-peak</b>	720	720	728	720	720
<b>Spring, peak</b>	1470	1470	1470	1470	1470
<b>Spring, off-peak</b>	736	736	736	736	736
<b>Summer, peak</b>	1472	1472	1472	1472	1472
<b>Summer, off-peak</b>	736	736	736	736	736
<b>Autumn, peak</b>	1456	1456	1456	1456	1456
<b>Autumn, off-peak</b>	728	728	728	728	728

Table 17 – Seasonal averaged peak/off-peak averaged EOC dataset,  $D_{SP}$ , period power price.

<b>Power price [Euro/MWh]</b>	<b>2010</b>	<b>2011</b>	<b>2012</b>	<b>2013</b>	<b>2014</b>
<b>Winter, peak</b>	55.11	51.29	46.21	40.09	32.95
<b>Winter, off-peak</b>	37.58	35.48	29.29	28.49	22.15
<b>Spring, peak</b>	45.49	56.95	37.08	42.97	31.62
<b>Spring, off-peak</b>	33.96	47.97	28.15	33.94	24.33
<b>Summer, peak</b>	48.85	50.75	39.44	46.76	34.01
<b>Summer, off-peak</b>	37.87	37.91	22.78	30.43	26.98
<b>Autumn, peak</b>	52.45	51.37	40.53	42.45	35.35
<b>Autumn, off-peak</b>	44.88	33.19	29.42	30.19	26.71

*Table 18 – Seasonal averaged peak/off-peak averaged EOC dataset,  $D_{SP}$ , period relative heat demand.*

<b>Relative heat demand[-]</b>	<b>2010</b>	<b>2011</b>	<b>2012</b>	<b>2013</b>	<b>2014</b>
<b>Winter, peak</b>	0.87	0.87	0.87	0.87	0.87
<b>Winter, off-peak</b>	0.73	0.73	0.73	0.73	0.73
<b>Spring, peak</b>	0.64	0.64	0.64	0.64	0.64
<b>Spring, off-peak</b>	0.45	0.45	0.45	0.45	0.45
<b>Summer, peak</b>	0.34	0.34	0.34	0.34	0.34
<b>Summer, off-peak</b>	0.15	0.15	0.15	0.15	0.15
<b>Autumn, peak</b>	0.62	0.62	0.62	0.62	0.62
<b>Autumn, off-peak</b>	0.36	0.36	0.36	0.36	0.36